



TECH BRIEFS

NATIONAL AERONAUTICS AND SPACE ADMINISTRATION

-  **Technology Focus**
-  **Electronics/Computers**
-  **Software**
-  **Materials**
-  **Mechanics/Machinery**
-  **Manufacturing**
-  **Bio-Medical**
-  **Physical Sciences**
-  **Information Sciences**
-  **Books and Reports**

INTRODUCTION

Tech Briefs are short announcements of innovations originating from research and development activities of the National Aeronautics and Space Administration. They emphasize information considered likely to be transferable across industrial, regional, or disciplinary lines and are issued to encourage commercial application.

Availability of NASA Tech Briefs and TSPs

Requests for individual Tech Briefs or for Technical Support Packages (TSPs) announced herein should be addressed to

National Technology Transfer Center

Telephone No. (800) 678-6882 or via World Wide Web at www2.nttc.edu/leads/

Please reference the control numbers appearing at the end of each Tech Brief. Information on NASA's Innovative Partnerships Program (IPP), its documents, and services is also available at the same facility or on the World Wide Web at <http://ipp.nasa.gov>.

Innovative Partnerships Offices are located at NASA field centers to provide technology-transfer access to industrial users. Inquiries can be made by contacting NASA field centers listed below.

NASA Field Centers and Program Offices

Ames Research Center

Lisa L. Lockyer
(650) 604-1754
lisa.l.lockyer@nasa.gov

Dryden Flight Research Center

Gregory Poteat
(661) 276-3872
greg.poteat@dfrc.nasa.gov

Glenn Research Center

Kathy Needham
(216) 433-2802
kathleen.k.needham@nasa.gov

Goddard Space Flight Center

Nona Cheeks
(301) 286-5810
nona.k.cheeks@nasa.gov

Jet Propulsion Laboratory

Ken Wolfenbarger
(818) 354-3821
james.k.wolfenbarger@jpl.nasa.gov

Johnson Space Center

Michele Brekke
(281) 483-4614
michele.a.brekke@nasa.gov

Kennedy Space Center

David R. Makufka
(321) 867-6227
david.r.makufka@nasa.gov

Langley Research Center

Martin Waszak
(757) 864-4015
martin.r.waszak@nasa.gov

Marshall Space Flight Center

Jim Dowdy
(256) 544-7604
jim.dowdy@msfc.nasa.gov

Stennis Space Center

John Bailey
(228) 688-1660
john.w.bailey@nasa.gov

Carl Ray, Program Executive

Small Business Innovation
Research (SBIR) & Small
Business Technology
Transfer (STTR) Programs
(202) 358-4652
carl.g.ray@nasa.gov

Doug Comstock, Director

Innovative Partnerships
Program Office
(202) 358-2560
doug.comstock@nasa.gov



TECH BRIEFS

NATIONAL AERONAUTICS AND SPACE ADMINISTRATION



5 Technology Focus: Test & Measurement

- 5 Charge-Control Unit for Testing Lithium-Ion Cells
- 6 Measuring Positions of Objects Using Two or More Cameras
- 7 Lidar System for Airborne Measurement of Clouds and Aerosols
- 8 Radiation-Insensitive Inverse Majority Gates
- 9 Reduced-Order Kalman Filtering for Processing Relative Measurements



11 Electronics/Computers

- 11 Spaceborne Processor Array
- 11 Instrumentation System Diagnoses a Thermocouple
- 12 Chromatic Modulator for a High-Resolution CCD or APS
- 13 Commercial Product Activation Using RFID
- 14 Cup Cylindrical Waveguide Antenna



15 Software

- 15 Aerobraking Maneuver (ABM) Report Generator
- 15 ABM Drag_Pass Report Generator
- 15 Transformation of OODT CAS To Perform Larger Tasks
- 15 Visualization Component of Vehicle Health Decision Support System
- 16 Mars Reconnaissance Orbiter Uplink Analysis Tool
- 16 Problem Reporting System
- 16 G-Guidance Interface Design for Small Body Mission Simulation
- 17 DSN Scheduling Engine
- 17 Replacement Sequence of Events Generator
- 17 Force-Control Algorithm for Surface Sampling
- 17 Tool for Merging Proposals Into DSN Schedules



19 Manufacturing & Prototyping

- 19 Micromachined Slits for Imaging Spectrometers
- 19 Fabricating Nanodots Using Lift-Off of a Nanopore Template
- 20 Making Complex Electrically Conductive Patterns on Cloth



21 Materials

- 21 Special Polymer/Carbon Composite Films for Detecting SO₂
- 21 Nickel-Based Superalloy Resists Embrittlement by Hydrogen
- 22 Chemical Passivation of Li⁺-Conducting Solid Electrolytes
- 23 Organic/Inorganic Polymeric Composites for Heat-Transfer Reduction
- 23 Composite Cathodes for Dual-Rate Li-Ion Batteries



25 Mechanics/Machinery

- 25 Improved Descent-Rate Limiting Mechanism
- 25 Alignment-Insensitive Lower-Cost Telescope Architecture
- 26 Micro-Resistojet for Small Satellites
- 26 Using Piezoelectric Devices To Transmit Power Through Walls
- 27 Miniature Latching Valve



29 Bio-Medical

- 29 Apparatus for Sampling Surface Contamination
- 29 Novel Species of Non-Spore-Forming Bacteria
- 30 Chamber for Aerosol Deposition of Bioparticles



31 Physical Sciences

- 31 Hyperspectral Sun Photometer for Atmospheric Characterization and Vicarious Calibrations
- 31 Dynamic Stability and Gravitational Balancing of Multiple Extended Bodies



33 Books & Reports

- 33 Simulation of Stochastic Processes by Coupled ODE-PDE
- 33 Cluster Inter-Spacecraft Communications
- 33 Genetic Algorithm Optimizes Q-LAW Control Parameters
- 33 Low-Impact Mating System for Docking Spacecraft
- 34 Non-Destructive Evaluation of Materials via Ultraviolet Spectroscopy
- 34 Gold-on-Polymer-Based Sensing Films for Detection of Organic and Inorganic Analytes in the Air
- 34 Quantum-Inspired Maximizer

This document was prepared under the sponsorship of the National Aeronautics and Space Administration. Neither the United States Government nor any person acting on behalf of the United States Government assumes any liability resulting from the use of the information contained in this document, or warrants that such use will be free from privately owned rights.



Charge-Control Unit for Testing Lithium-Ion Cells

This unit is useful for testing any non-aerospace battery cells.

John H. Glenn Research Center, Cleveland, Ohio

A charge-control unit was developed as part of a program to validate Li-ion cells packaged together in batteries for aerospace use. The lithium-ion cell charge-control unit will be useful to anyone who performs testing of battery cells for aerospace and non-aerospace uses and to anyone who manufactures battery test equipment. This technology reduces the quantity of costly power supplies and independent channels that are needed for test programs in which multiple cells are tested. The cost savings that were achieved in a test program are shown in Figure 1. Battery test equipment manufacturers can integrate the technology into their battery test equipment as a method to manage charging of multiple cells in series.

The unit manages a complex scheme that is required for charging Li-ion cells electrically connected in series. The unit makes it possible to evaluate cells together as a pack using a single primary test channel, while also making it possible to charge each cell individually. Hence, inherent cell-to-cell variations in a series string of cells can be addressed, and yet the cost of testing is reduced substantially below the cost of testing each cell as a separate entity.

In the original aerospace application, life-test data on Li-ion cells is critical in order to assess their performances and capabilities relevant to NASA missions and exploration goals. For example, for many NASA missions that involve flight in low orbits around the Earth, batteries are required to endure more than 30,000 charge/discharge cycles, and Li-ion batteries are relatively new to this type of application. The scheme required for charging Li-ion cells is more complex than that typically required for charging the alkaline cells that the Li-ion cells may supplant. This scheme includes the establishment and enforcement of strict cell voltage limits to ensure safe, long operation.

So that this requirement could be addressed in laboratory testing, the present charge-control unit was developed to manage the current through each

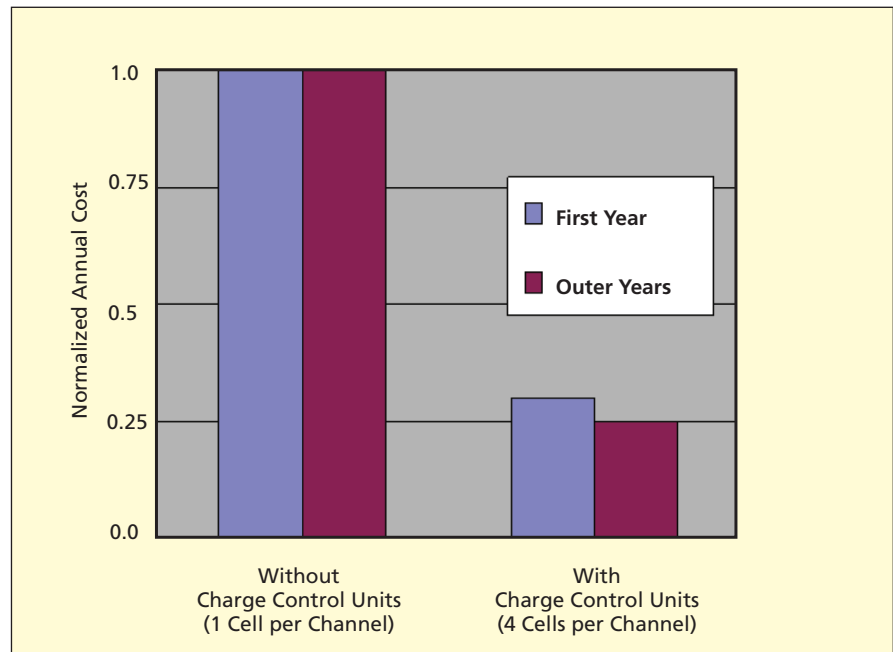


Figure 1. A Comparison of the Annual Costs of a three-year battery cell test program is shown without charge control units and with charge control units (escalation is neglected). The first year costs include the capital cost of the charge control units.

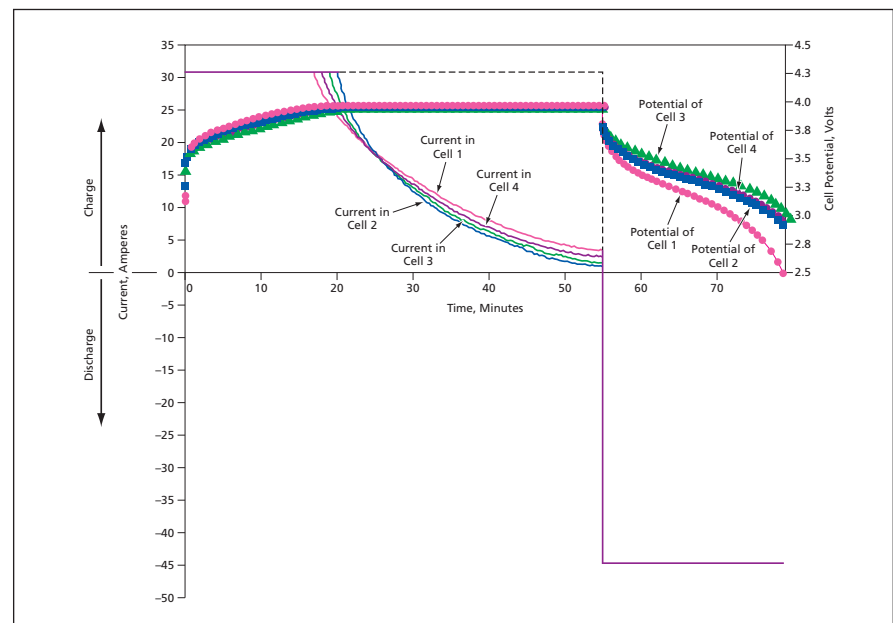


Figure 2. These Current and Voltage Plots represent measurements on four series-connected, unmatched Li-ion cells that were charged by use of the present charge-control unit for 55 minutes, then discharged.

cell once the voltage of the cell reaches the established limit. By use of this unit, multiple Li-ion cells connected in series within a battery pack can be charged from a single current source, and yet the charging of each cell is controlled independently of the other cells. More specifically, by use of this unit:

- Each cell in the series string is charged at full current until the cell voltage reaches the limit;
- Once the voltage of a given cell reaches the limit, the voltage is held at that limit and the current through that cell is tapered off so that the cell continues to gain some charge without becoming overcharged; and

- Even after some cells have reached voltage limit, other cells that are at lower states of charge continue to be charged at full current until they reach the voltage limit (see Figure 2).

The unit consists of electronic circuits and thermal-management devices housed in a common package. It also includes isolated annunciators to signal when the cells are being actively bypassed. These annunciators can be used by external charge managers or can be connected in series to signal that all cells have reached maximum charge. The charge-control circuitry for each cell amounts to regulator circuitry and is powered by that cell, eliminating the need for an external power source or

controller. A 110-VAC source of electricity is required to power the thermal-management portion of the unit. A small direct-current source can be used to supply power for an annunciator signal, if desired.

This work was done by Concha M. Reid, Michelle A. Manzo, and Robert M. Button of Glenn Research Center and Russel Gemeiner of QSS Group, Inc. Further information is contained in a TSP (see page 1).

Inquiries concerning rights for the commercial use of this invention should be addressed to NASA Glenn Research Center, Innovative Partnerships Office, Attn: Steve Fedor, Mail Stop 4-8, 21000 Brookpark Road, Cleveland, Ohio 44135. Refer to LEW-17703-1.

➤ Measuring Positions of Objects Using Two or More Cameras

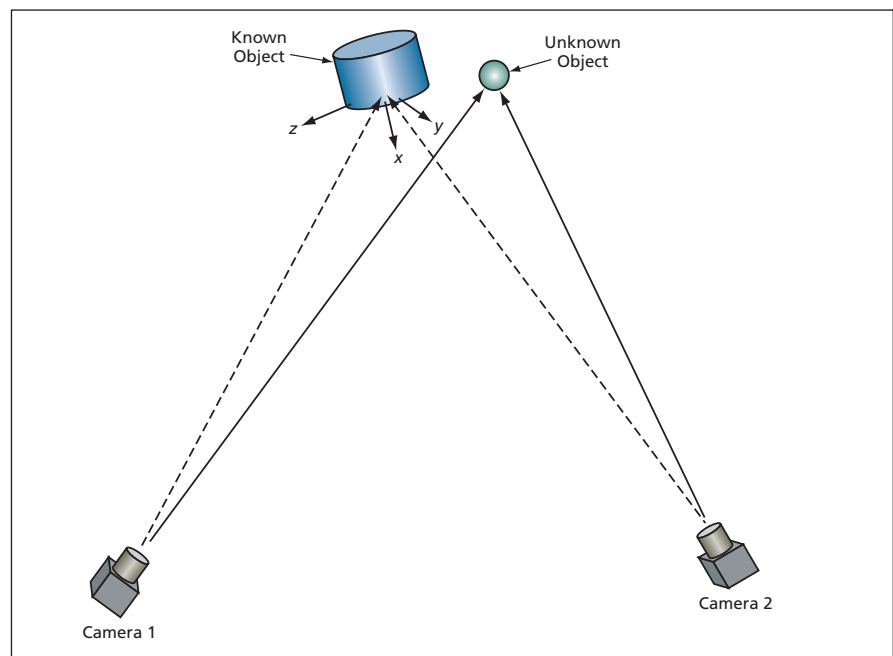
This method could determine the causes of accidents.

John F. Kennedy Space Center, Florida

An improved method of computing positions of objects from digitized images acquired by two or more cameras (see figure) has been developed for use in tracking debris shed by a spacecraft during and shortly after launch. The method is also readily adaptable to such applications as (1) tracking moving and possibly interacting objects in other settings in order to determine causes of accidents and (2) measuring positions of stationary objects, as in surveying. Images acquired by cameras fixed to the ground and/or cameras mounted on tracking telescopes can be used in this method.

In this method, processing of image data starts with creation of detailed computer-aided design (CAD) models of the objects to be tracked. By rotating, translating, resizing, and overlaying the models with digitized camera images, parameters that characterize the position and orientation of the camera can be determined. The final position error depends on how well the centroids of the objects in the images are measured; how accurately the centroids are interpolated for synchronization of cameras; and how effectively matches are made to determine rotation, scaling, and translation parameters.

The method involves use of the perspective camera model (also denoted the point camera model), which is one of several mathematical models developed over the years to represent the relationships between external coordinates of objects and the coordinates of



Two Cameras Are Aimed at a pair of possibly moving objects, at least one of which is known. The positions and orientations of the cameras relative to the known object need not be known initially; instead, they are determined by means of photogrammetric computations.

the objects as they appear on the image plane in a camera. The point camera model is implemented in a commercially available software system for three-dimensional graphics and animation used in television, film, industrial design, architecture, and medical imaging.

The method also involves extensive use of the affine camera model, in which the distance from the camera to an object (or

to a small feature on an object) is assumed to be much greater than the size of the object (or feature), resulting in a truly two-dimensional image. Using a technique common in photogrammetry as practiced in aerial surveying, depth information is obtained from a combination of image data acquired from two or more cameras. Synchronized image data from two or more cameras are combined

following an error-minimization approach. Precise measurements are obtained by synchronizing data by use of linear interpolation and a dual-camera trajectory solution. Velocities of objects are also estimated in this model.

The affine camera model does not require advance knowledge of the positions and orientations of the cameras. This is because ultimately, positions and orientations of the cameras and of all

objects are computed in a coordinate system attached to one object as defined in its CAD model.

Initially, the software developed to solve the equations of the affine camera model implemented a gradient-descent algorithm for finding a solution of a matrix-vector equation that minimizes an error function. Whereas photogrammetric analyses typically entailed weeks of measurements and computations to obtain ac-

curate results from a given set of images, this software yielded solutions in times of the order of minutes. A more recent version of the software solves the affine-camera-model equations directly by means of a matrix inversion in a typical computation time of the order of a second.

This work was done by Steve Klinko, John Lane, and Christopher Nelson of ASRC Aerospace for Kennedy Space Center. KSC-12665/3/705

Lidar System for Airborne Measurement of Clouds and Aerosols

This is an eye-safe, rugged, all-solid-state system.

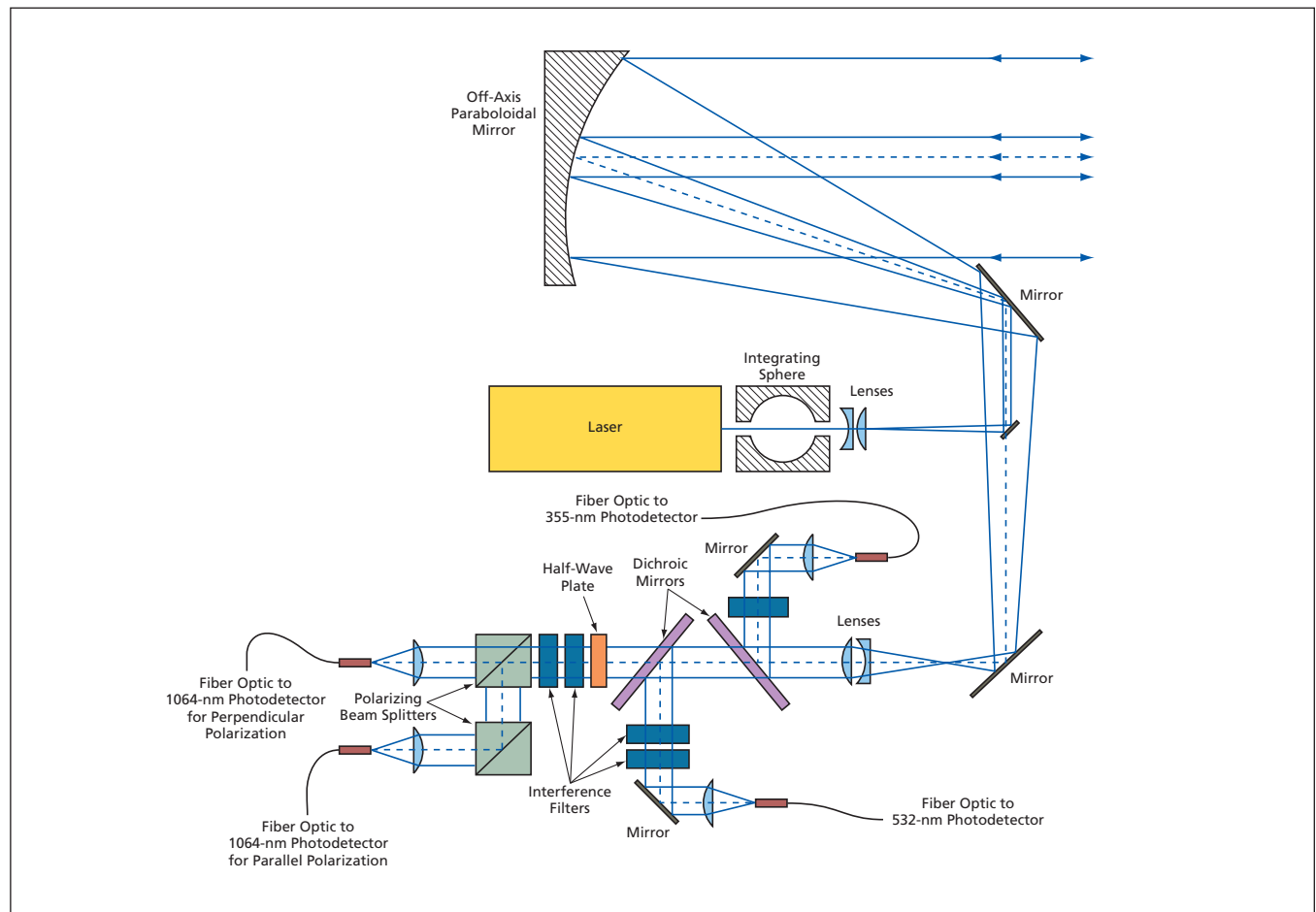
Goddard Space Flight Center, Greenbelt, Maryland

The figure schematically depicts a lidar system for measuring optical properties of clouds and aerosols at three wavelengths. The system is designed to be operated aboard the NASA ER-2 aircraft, which typically cruises at an altitude of about 20 km — above about 94 percent of the mass of the atmosphere. The sys-

tem can also be operated aboard several other aircraft, and a version for use on Unmanned Aerial Vehicles (UAVs) is presently under construction. In addition to the requirement for fully autonomous operation in a demanding airborne environment, three other main requirements have governed the design: (1) to make

the system eye-safe at the operating altitude; (2) to make the system as lightweight as possible, yet rugged; and (3) to use solid-state photon-counting detectors fiber-coupled to the receiver.

The laser transmitter is based on a Nd:YVO₄ laser crystal pumped by light coupled to the crystal via optical fibers



This **Simplified Optical Layout** (not to scale) shows the main optical components of a lidar system designed for measuring selected optical properties of clouds and aerosols at three wavelengths.

from laser diodes that are located away from the crystal to aid in dissipating the heat generated in the diodes and their drive circuits. The output of the Nd:YVO₄ crystal has a wavelength of 1064 nm, and is made to pass through frequency-doubling and frequency-tripling crystals. As a result, the net laser output is a collinear superposition of beams at wavelengths of 1064, 532, and 355 nm.

The laser operates at a pulse-repetition rate of 5 kHz, emitting per-pulse energies of 50 μJ at 1064 nm, 25 μJ at 532 nm, and 50 μJ at 355 nm. The transmitted laser beam and the returning laser light backscattered from atmospheric aerosols and molecules pass through a telescope, the primary optical element of which is an off-axis parabolic mirror having an aperture diameter of 20 cm. The combination of the off-axis arrangement and other features is such that none of the transmitting aperture is obscured and only about 20 percent of the receiving aperture is obscured.

The returning light collected by the telescope is separated into wavelength components by use of dichroics and nar-

rowband interference filters suppress solar background. The 1064-nm signal is further separated into parallel and perpendicular polarization components. A half-wave plate is inserted in the 1064-nm path to enable calibration of the parallel- and perpendicular-polarization channels. Each resulting output wavelength component is coupled via an optical fiber to a photodetector.

An important feature of this system is an integrating sphere located between the laser output and the laser beam expander lenses. The integrating sphere collects light scattered from the lenses. Three energy-monitor detectors are located at ports inside the integrating sphere. Each of these detectors is equipped with filters such that the laser output energy is measured independently for each wavelength. The laser output energy is measured on each pulse to enable the most accurate calibration possible.

The 1064-nm and 532-nm photodetectors are, more specifically, single-photon-counting modules (SPCMs). When used at 1064 nm, these detectors have approximately 3 percent quantum efficiency and low thermal noise (fewer

than 200 counts per second). When used at 532 nm, the SPCMs have quantum efficiency of about 60 percent. The photodetector for the 355-nm channel is a photon-counting photomultiplier tube having a quantum efficiency of about 20 percent.

The use of photon-counting detectors is made feasible by the low laser pulse energy. The main advantage of photon-counting (in contradistinction to processing of analog photodetector outputs) is ease of inversion of data without need for complicated calibration schemes like those necessary for analog detectors. The disadvantage of photon-counting detectors is that they inherently have narrow dynamic ranges. However, by using photon-counting detectors along with a high-repetition-rate laser, it is possible to obtain wide dynamic range through accumulation of counts over many pulses.

This work was done by Matthew McGill and V. Stanley Scott of Goddard Space Flight Center, Luis Ramos Izquierdo of LRI Corp., and Joe Marzouk of Sigma Space Corp. Further information is contained in a TSP (see page 1). GSC-14985-1

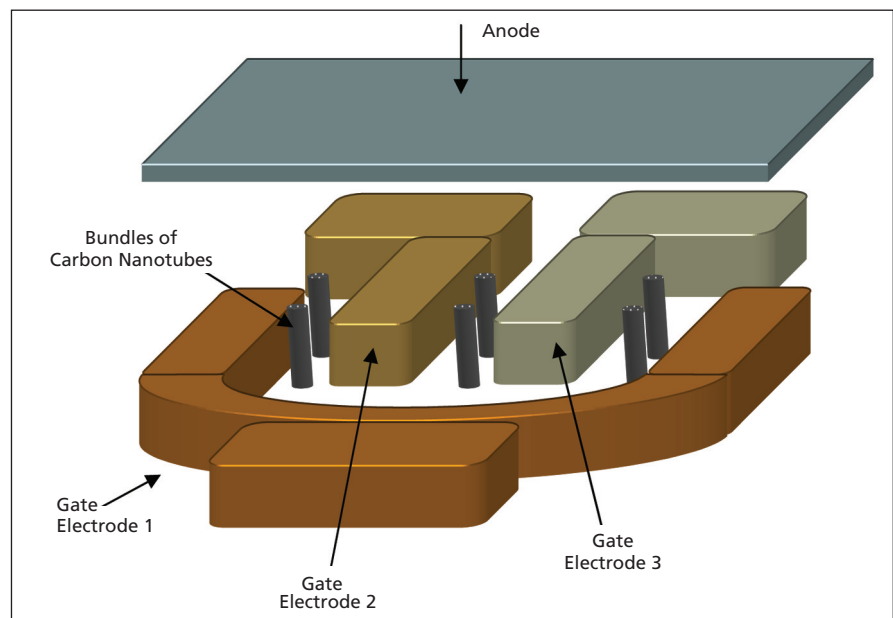
Radiation-Insensitive Inverse Majority Gates

These gates would be implemented as microscopic vacuum electronic devices.

NASA's Jet Propulsion Laboratory, Pasadena, California

To help satisfy a need for high-density logic circuits insensitive to radiation, it has been proposed to realize inverse majority gates as microscopic vacuum electronic devices. In comparison with solid-state electronic devices ordinarily used in logic circuits, vacuum electronic devices are inherently much less adversely affected by radiation and extreme temperatures.

The proposed development would involve state-of-the-art micromachining and recent advances in the fabrication of carbon-nanotube-based field emitters. A representative three-input inverse majority gate (see figure) would be a monolithic, integrated structure that would include three gate electrodes, six bundles of carbon nanotubes (serving as electron emitters) at suitable positions between the gate electrodes, and an overhanging anode. The bundles of carbon nanotubes would be grown on degenerately doped silicon substrates that would be parts of the monolithic structure. The gate electrodes would be fabricated



A **Three-Input Inverse Majority Gate** as proposed would be a microscopic vacuum electronic device containing bundles of carbon nanotubes positioned between gate electrodes to obtain controlled field emission of electrons from the bundles. In the presence of a fixed positive bias potential on the anode, the application of suitable (possibly smaller) bias potential to any two or all three gate electrodes would divert all the electron current from the anode.

as parts of the monolithic structure by means of a double-silicon-on-insulator process developed at NASA's Jet Propulsion Laboratory. The tops of the bundles of carbon nanotubes would lie below the plane of the tops of the gate electrodes. The particular choice of shapes, dimensions, and relative positions of the electrodes and bundles of carbon nanotubes would provide for both field emission of electrons from the bundles of carbon nanotubes and control of the electron current to obtain the inverse majority function, as described next.

The application of a positive bias potential to the anode would cause emission of electrons from the bundles of carbon nanotubes and, if no bias potential were applied to the gate electrodes, the electrons would travel to the anode, giving rise to an anode current. Relative to the anode, the gate electrodes would be much closer to the bundles of carbon nanotubes, such that the application of a smaller positive bias potential to a gate

electrode would suffice to divert, to that electrode, the electrons emitted by the adjacent bundles of carbon nanotubes.

If the positive bias potential were not applied to another gate electrode, then the anode would continue to draw an electron current from the bundles of carbon nanotubes not adjacent to the positively biased gate electrode. However, if the positive bias potential were applied to any two or all three of the gate electrodes, then all of the electrons emitted by all the bundles of carbon nanotubes would be diverted to the positively biased gate electrodes, causing the anode current to fall to zero. In terms of binary logic, if one regards nonzero anode current as representing output state 1, zero anode current as representing output state 0, positive gate-electrode bias as representing input state 1, and zero gate-electrode bias as representing input state 0, then logical 0 inputs to two or all three of gate terminals would result in output of

logical 1, and logical 1 inputs to two or all three of the gate terminals would result in output of logical 0. This relationship among input and output states constitutes a NAND and a NOR gate combination. This is the inverse majority function.

This work was done by Harish Manohara and Mohammad Mojarradi of Caltech for NASA's Jet Propulsion Laboratory. Further information is contained in a TSP (see page 1).

In accordance with Public Law 96-517, the contractor has elected to retain title to this invention. Inquiries concerning rights for its commercial use should be addressed to:

*Innovative Technology Assets Management
JPL
Mail Stop 202-233
4800 Oak Grove Drive
Pasadena, CA 91109-8099
E-mail: iaoffice@jpl.nasa.gov
Refer to NPO-45388 volume and number of this NASA Tech Briefs issue, and the page number.*

➤ Reduced-Order Kalman Filtering for Processing Relative Measurements

A Kalman filter can be propagated using fewer computations.

NASA's Jet Propulsion Laboratory, Pasadena, California

A study in Kalman-filter theory has led to a method of processing relative measurements to estimate the current state of a physical system, using less computation than has previously been thought necessary. As used here, "relative measurements" signifies measurements that yield information on the relationship between a later and an earlier state of the system. An important example of relative measurements arises in computer vision: Information on relative motion is extracted by comparing images taken at two different times.

Relative measurements do not directly fit into standard Kalman filter theory, in which measurements are restricted to those indicative of only the current state of the system. One approach heretofore followed in utilizing relative measurements in Kalman filtering, denoted state augmentation, involves augmenting the state of the system at the earlier of two

time instants and then propagating the state to the later time instant. While state augmentation is conceptually simple, it can also be computationally prohibitive because it doubles the number of states in the Kalman filter.

In many practical applications, relative measurements are not functions of entire earlier states but rather may be a function of only a subset of elements of the earlier state. A relative measurement that can be thus characterized is denoted a partial relative measurement. For example, in computer vision, relative-measurement information is usually a function of position rather than velocity, acceleration, or other elements of the state.

When processing a relative measurement, if one were to follow the state-augmentation approach as practiced heretofore, one would find it necessary to propagate the full augmented state

Kalman filter from the earlier time to the later time and then select out the reduced-order components. The main result of the study reported here is proof of a property called reduced-order equivalence (ROE). The main consequence of ROE is that it is not necessary to augment with the full state, but, rather, only the portion of the state that is explicitly used in the partial relative measurement. In other words, it suffices to select the reduced-order components first and then propagate the partial augmented state Kalman filter from the earlier time to the later time; the amount of computation needed to do this can be substantially less than that needed for propagating the full augmented Kalman state filter.

This work was done by David S. Bayard of Caltech for NASA's Jet Propulsion Laboratory. For more information, contact iaoffice@jpl.nasa.gov. NPO-44427



Spaceborne Processor Array

NASA's Jet Propulsion Laboratory, Pasadena, California

A Spaceborne Processor Array in Multifunctional Structure (SPAMS) can lower the total mass of the electronic and structural overhead of spacecraft, resulting in reduced launch costs, while increasing the science return through dynamic onboard computing. SPAMS integrates the multifunctional structure (MFS) and the Gilgamesh Memory, Intelligence, and Network Device (MIND) multi-core in-memory computer architecture into a single-system super-architecture. This transforms every inch of a spacecraft into a sharable, interconnected, smart computing element to increase computing performance while simultaneously reducing mass.

The MIND in-memory architecture provides a foundation for high-performance, low-power, and fault-tolerant com-

puting. The MIND chip has an internal structure that includes memory, processing, and communication functionality. The Gilgamesh is a scalable system comprising multiple MIND chips interconnected to operate as a single, tightly coupled, parallel computer. The array of MIND components shares a global, virtual name space for program variables and tasks that are allocated at run time to the distributed physical memory and processing resources. Individual processor-memory nodes can be activated or powered down at run time to provide active power management and to configure around faults.

A SPAMS system is comprised of a distributed Gilgamesh array built into MFS, interfaces into instrument and communication subsystems, a mass storage in-

terface, and a radiation-hardened flight computer.

This work was done by Edward T. Chow, Donald V. Schatzel, and William D. Whitaker of Caltech and Thomas Sterling of Louisiana State University for NASA's Jet Propulsion Laboratory.

In accordance with Public Law 96-517, the contractor has elected to retain title to this invention. Inquiries concerning rights for its commercial use should be addressed to:

*Innovative Technology Assets Management
JPL*

*Mail Stop 202-233
4800 Oak Grove Drive
Pasadena, CA 91109-8099*

E-mail: iaoffice@jpl.nasa.gov

Refer to NPO-44023, volume and number of this NASA Tech Briefs issue, and the page number.

Instrumentation System Diagnoses a Thermocouple

This system can detect an open or short circuit or a debond.

John F. Kennedy Space Center, Florida

An improved self-validating thermocouple (SVT) instrumentation system not only acquires readings from a thermocouple but is also capable of detecting deterioration and a variety of discrete faults in the thermocouple and its lead wires. Prime examples of detectable discrete faults and deterioration include open- and short-circuit conditions and debonding of the thermocouple junction from the object, the temperature of which one seeks to measure. Debonding is the most common cause of errors in thermocouple measurements, but most prior SVT instrumentation systems have not been capable of detecting debonding.

The improved SVT instrumentation system includes power circuitry, a cold-junction compensator, signal-conditioning circuitry, pulse-width-modulation (PWM) thermocouple-excitation circuitry, an analog-to-digital converter (ADC), a digital data processor, and a universal serial bus (USB) interface. The system can operate in any of the follow-

ing three modes:

- *Temperature Measurement*

In this mode, the ADC samples the output voltages of the thermocouple and the cold-junction compensator. Because the output voltage of the thermocouple is very small (typically of the order of microvolts or millivolts), it is necessary to utilize the gain of the ADC. The processor uses the cold-junction-compensator reading to obtain a compensated thermocouple output voltage, V_{out} , then calculates the temperature at the thermocouple tip by use of the equa-

$$T_{tip} = \sum_{k=0}^n A_k V_{out}^k$$

tion of the form

where the A_k s are calibration parameters, V_{out} is the compensated thermocouple output voltage, and k and n are integers.

- *Thermocouple Validation*

For the purpose of determining whether there is a short or open circuit,

the two thermocouple leads are subjected to a common-mode DC excitation or, via capacitors, to a differential-mode PWM excitation. From the response to the DC excitation, the processor can determine whether or not there is a short circuit. From response to the PWM excitation, the processor can determine whether there is an open circuit.

- *Bonding/Debonding Detection*

The processor commands the application of a PWM excitation, via a capacitor, to the thermocouple for a certain amount of time to heat the thermocouple. (Inductors in the thermocouple leads prevent the PWM excitation from reaching the thermocouple cold junction.) The characteristic time or rate of increase in temperature during the excitation is analyzed by the processor as an indication of the integrity of the thermocouple. The characteristic time or rate of decay of the temperature after the excitation is analyzed by the processor as an indication of the thermal resistance (and, hence, of bonding or debonding)

between the thermocouple and the object, the temperature of which one seeks to measure.

The software running in the processor includes components that implement statistical algorithms to evaluate the state of the thermocouple and the instrumentation system. When power is first turned on, the user can elect to start a diagnosis/monitoring sequence, in which the

PWM is used to estimate the characteristic times corresponding to the correct configuration. The user also has the option of using previous diagnostic values, which are stored in an electrically erasable, programmable read-only memory so that they are available every time the power is turned on.

This work was done by Jose Perotti and Josephine Santiago of Kennedy Space Center

and Carlos Mata, Peter Vokrot, Carlos Zavala, and Bradley Burns of ASRC Aerospace Corp.

This invention is owned by NASA, and a patent application has been filed. Inquiries concerning nonexclusive or exclusive license for its commercial development should be addressed to the Kennedy Innovative Partnerships Office at (321) 861-7158. Refer to KSC-12875.

Chromatic Modulator for a High-Resolution CCD or APS

Color images would be detected without loss of spatial resolution.

NASA's Jet Propulsion Laboratory, Pasadena, California

A chromatic modulator has been proposed to enable the separate detection of the red, green, and blue (RGB) color components of the same scene by a single charge-coupled device (CCD), active-pixel sensor (APS), or similar electronic image detector. Traditionally, the RGB color-separation problem in an electronic camera has been solved by use of either (1) fixed color filters over three separate image detectors; (2) a filter wheel that repeatedly imposes a red, then a green, then a blue filter over a single image detector; or (3) different

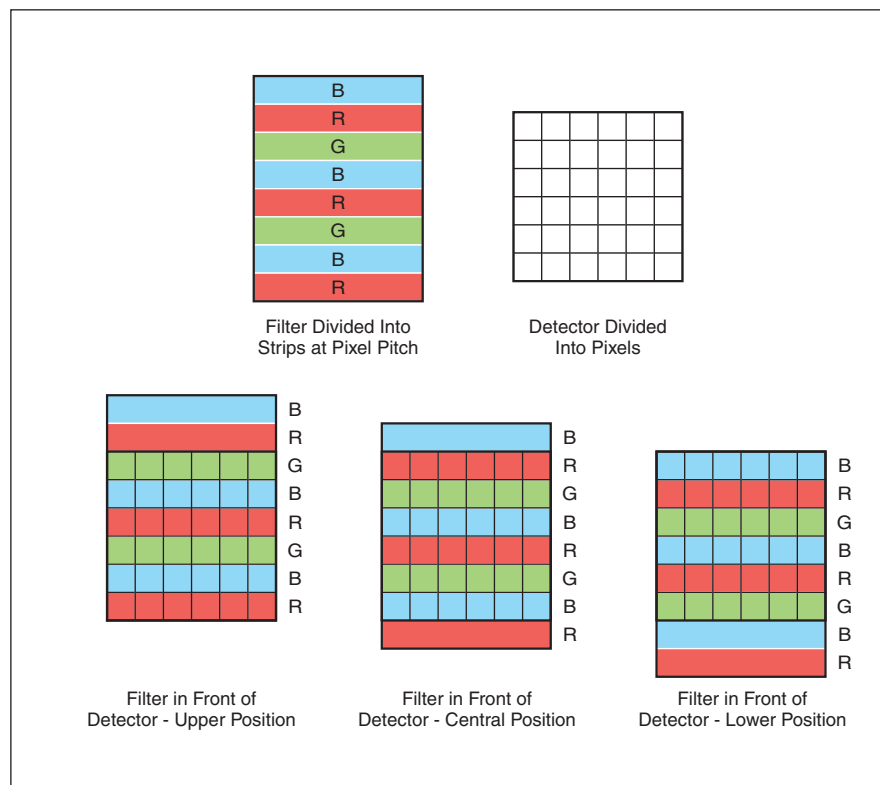
fixed color filters over adjacent pixels. The use of separate image detectors necessitates precise registration of the detectors and the use of complicated optics; filter wheels are expensive and add considerably to the bulk of the camera; and fixed pixelated color filters reduce spatial resolution and introduce color-aliasing effects. The proposed chromatic modulator would not exhibit any of these shortcomings.

The proposed chromatic modulator would be an electromechanical device fabricated by micromachining. It would

include a filter having a spatially periodic pattern of RGB strips at a pitch equal to that of the pixels of the image detector (see figure). The filter would be placed in front of the image detector, supported at its periphery by a spring suspension and electrostatic comb drive. The spring suspension would bias the filter toward a middle position in which each filter strip would be registered with a row of pixels of the image detector. Hard stops would limit the excursion of the spring suspension to precisely one pixel row above and one pixel row below the middle position.

In operation, the electrostatic comb drive would be actuated to repeatedly snap the filter to the upper extreme, middle, and lower extreme positions. This action would repeatedly place a succession of the differently colored filter strips in front of each pixel of the image detector. At each filter position, each detector pixel would thus acquire information on the local brightness in the momentarily selected color. The frequency of actuation of the comb drive would be three times the frame rate of the camera, so that over one frame period, each pixel would acquire full color information. Hence, the camera would acquire full color information at full pixel resolution.

Of course, it would be necessary to time-multiplex the outputs of the pixels for processing in a manner consistent with the spatial and temporal periodicity of the color information acquired by each detector pixel. To simplify the processing, it would be desirable to encode information on the color of the filter strip over each row (or at least over some representative rows) of pixels at a given instant of time in synchronism with the pixel output at that instant. This could be accom-



Red, Green, and Blue Filter Strips would be registered with pixel rows in a repeating pattern. The filter would be repeatedly placed in the upper, middle, and lower positions to repeatedly expose each pixel to each color.

plished by means of an alternating pattern of opaque patches over the last two pixel-column positions of each filter strip: for example, nonzero illumination at both of these column positions could signify the presence of the red filter strip, zero illumination at one of these column

positions could signify the presence of the green filter strip, and zero illumination at both of these column positions could signify the presence of the blue filter strip.

This work was done by Frank Hartley and Anthony Hull of Caltech for NASA's Jet Propulsion Laboratory.

This invention is owned by NASA, and a patent application has been filed. Inquiries concerning nonexclusive or exclusive license for its commercial development should be addressed to the Patent Counsel, NASA Management Office-JPL. Refer to NPO-20896.

Commercial Product Activation Using RFID

Products would be tracked to points of sale and there activated automatically.

NASA's Jet Propulsion Laboratory, Pasadena, California

Radio-frequency identification (RFID) would be used for commercial product activation, according to a proposal. The concept of RFID is not new: RFID systems are widely used in commerce for tracking such diverse assets as animals, credit cards, and retail products. Also not new is the concept of manufacturing commercial products to be nonfunctional or unusable until activated at points of sale or in response to electronic submission of proof of purchase. What is new here is the concept of combining RFID with activation — more specifically, using RFID for activating commercial products (principally, electronic ones) and for performing such ancillary functions as tracking individual product units on production lines, tracking shipments, and updating inventories (see figure).

According to the proposal, an RFID chip would be embedded in each product. The information encoded in the chip would include a unique number for identifying the product. An RFID reader at the point of sale would record the number of the product and would write digital information to the RFID chip for either immediate activation of the product or for later interrogation and processing.

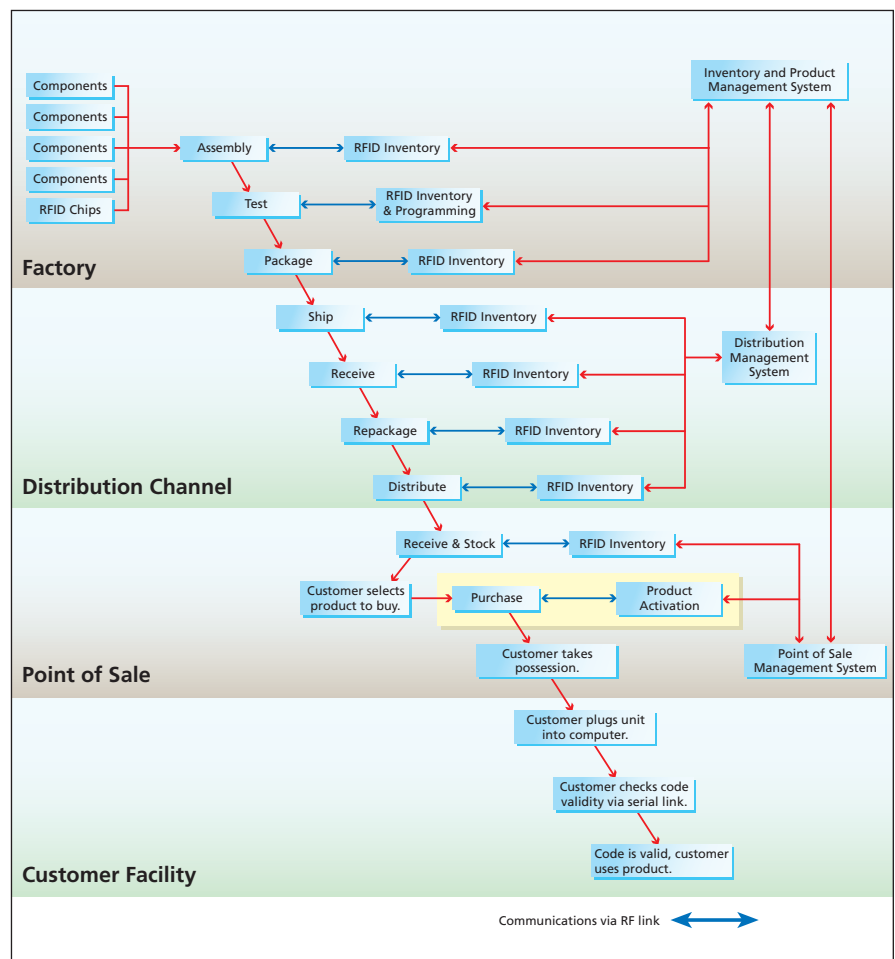
To be practical, an RFID product-activation system should satisfy a number of key requirements:

- The system should be designed to be integrable into the inventory-tracking and the data-processing and -communication infrastructures of businesses along the entire supply chain from manufacture to retail.
- The system should be resistant to sophisticated hacking.
- Activation codes should be made sufficiently complex to minimize the probability of activating stolen products.
- RFID activation equipment at points of sale must be capable of two-way RF communication for the purposes of

reading information from, and writing information to, embedded RFID chips.

- The equipment at points of sale should be easily operable by sales clerks with little or no training.
- The point-of-sale equipment should verify activation and provide visible and/or audible signals indicating verification or the lack thereof.
- The system should be able to handle millions of products per year with minimal human intervention.

- The system should support non-simultaneous dual data-communication interfaces: (1) the RF link between the product-activation infrastructure and the RFID chip in each product and (2) a serial link, within each product, between the RFID chip and a control circuit.
- To the extent possible, the system should be constructed using relatively inexpensive off-the-shelf RFID equipment and methods that conform to in-



An RFID Chip embedded in each product at manufacture would be used to track the product through the entire supply chain and would be used to activate the product at the point of sale.

ternational standards and that involve minimal additions to pre-existing manufacturing processes and facilities.

- RFID chips should not contain batteries: instead, they should derive power from interrogating RF fields.

This work was done by Thomas Jedrey and Eric Archer of Caltech for NASA's Jet Propul-

sion Laboratory. Further information is contained in a TSP (see page 1).

In accordance with Public Law 96-517, the contractor has elected to retain title to this invention. Inquiries concerning rights for its commercial use should be addressed to:

*Innovative Technology Assets Management
JPL*

*Mail Stop 202-233
4800 Oak Grove Drive
Pasadena, CA 91109-8099
(818) 354-2240*

*E-mail: iaoffice@jpl.nasa.gov
Refer to NPO-42633, volume and number of this NASA Tech Briefs issue, and the page number.*

Cup Cylindrical Waveguide Antenna

This antenna is used in wireless networks and telemetry.

John H. Glenn Research Center, Cleveland, Ohio

The cup cylindrical waveguide antenna (CCWA) is a short backfire microwave antenna capable of simultaneously supporting the transmission or reception of two distinct signals having opposite circular polarizations. Short backfire antennas are widely used in mobile/satellite communications,

tracking, telemetry, and wireless local area networks because of their compactness and excellent radiation characteristics.

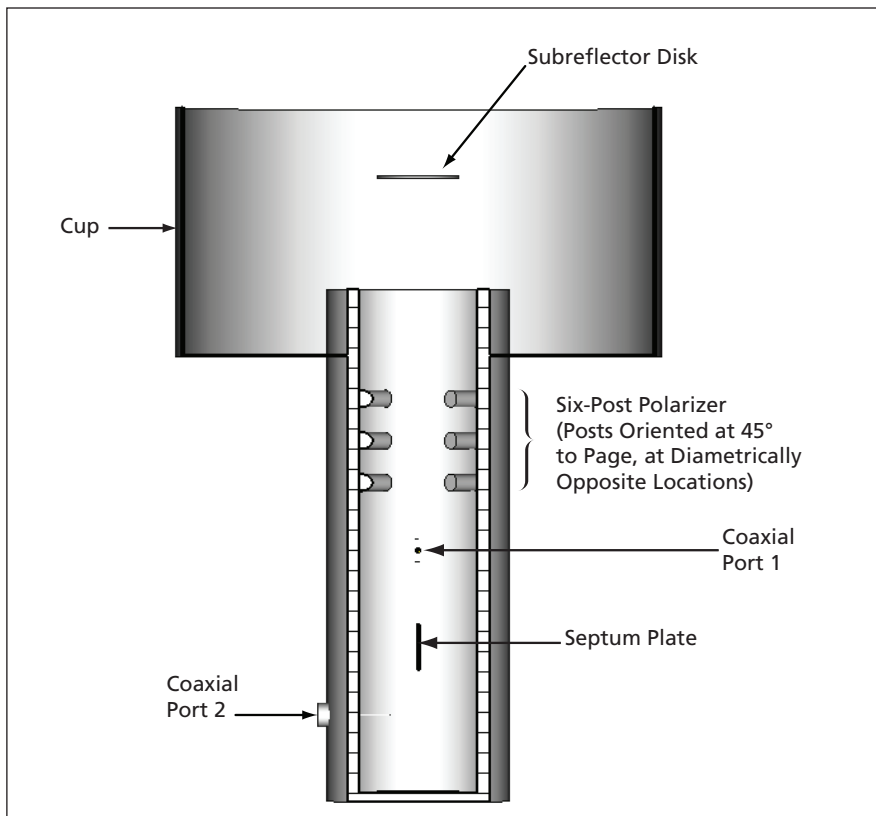
A typical prior short backfire antenna contains a half-wavelength dipole excitation element for linear polarization or crossed half-wavelength dipole ele-

ments for circular polarization. In order to achieve simultaneous dual circular polarization, it would be necessary to integrate, into the antenna feed structure, a network of hybrid components, which would introduce significant losses. The CCWA embodies an alternate approach that entails relatively low losses and affords the additional advantage of compactness.

The CCWA (see figure) includes a circular cylindrical cup, a circular disk subreflector, and a circular waveguide that serves as the excitation element. The components that make it possible to obtain simultaneous dual circular polarization are integrated into the circular waveguide. These components are a six-post polarizer and an orthomode transducer (OMT) with two orthogonal coaxial ports. The overall length of the OMT and polarizer (for the nominal design frequency of 2.25 GHz) is about 11 in. (≈ 28 cm), whereas the length of a commercially available OMT and polarizer for the same frequency is about 32 in. (≈ 81 cm).

This work was done by Roberto J. Acosta and William G. Darby of Glenn Research Center and Carol L. Kory, Kevin M. Lambert, and Daniel P. Breen of Analex Corp. Further information is contained in a TSP (see page 1).

Inquiries concerning rights for the commercial use of this invention should be addressed to NASA Glenn Research Center, Innovative Partnerships Office, Attn: Steve Fedor, Mail Stop 4-8, 21000 Brookpark Road, Cleveland, Ohio 44135. Refer to LEW-18089-1.



The Cup Cylindrical Waveguide Antenna features a compact combination of a polarizer and an orthomode transducer with two coaxial ports integrated into a circular waveguide.



🔍 Aerobraking Maneuver (ABM) Report Generator

abmREPORT Version 3.1 is a Perl script that extracts vital summarization information from the Mars Reconnaissance Orbiter (MRO) aerobraking ABM build process. This information facilitates sequence reviews, and provides a high-level summarization of the sequence for mission management.

The script extracts information from the ENV, SSF, FRF, SCMFmax, and OPTG files and burn magnitude configuration files and presents them in a single, easy-to-check report that provides the majority of the parameters necessary for cross check and verification during the sequence review process. This means that needed information, formerly spread across a number of different files and each in a different format, is all available in this one application. This program is built on the capabilities developed in dragReport and then the scripts evolved as the two tools continued to be developed in parallel.

This program was written by Forest Fisher, Roy Gladden, and Teerapat Khanamornpan of Caltech for NASA's Jet Propulsion Laboratory.

This software is available for commercial licensing. Please contact Karina Edmonds of the California Institute of Technology at (626) 395-2322. Refer to NPO-44382.

🔍 ABM Drag_Pass Report Generator

dragREPORT software was developed in parallel with abmREPORT, which is described in the preceding article. Both programs were built on the capabilities created during that process. This tool generates a drag_pass report that summarizes vital information from the MRO aerobraking drag_pass build process to facilitate both sequence reviews and provide a high-level summarization of the sequence for mission management. The script extracts information from the ENV, SSF, FRF, SCMFmax, and OPTG files, presenting them in a single, easy-to-check report providing the majority of parameters needed for cross check and verification as part of the sequence review process.

Prior to dragReport, all the needed information was spread across a number

of different files, each in a different format. This software is a Perl script that extracts vital summarization information and build-process details from a number of source files into a single, concise report format used to aid the MPST sequence review process and to provide a high-level summarization of the sequence for mission management reference. This software could be adapted for future aerobraking missions to provide similar reports, review and summarization information.

This program was written by Forest Fisher, Roy Gladden, and Teerapat Khanamornpan of Caltech for NASA's Jet Propulsion Laboratory.

This software is available for commercial licensing. Please contact Karina Edmonds of the California Institute of Technology at (626) 395-2322. Refer to NPO-44384.

🔍 Transformation of OODT CAS To Perform Larger Tasks

A computer program denoted OODT CAS has been transformed to enable performance of larger tasks that involve greatly increased data volumes and increasingly intensive processing of data on heterogeneous, geographically dispersed computers. Prior to the transformation, OODT CAS (also alternatively denoted, simply, "CAS") [wherein "OODT" signifies "Object-Oriented Data Technology" and "CAS" signifies "Catalog and Archive Service"] was a proven software component used to manage scientific data from spaceflight missions. In the transformation, CAS was split into two separate components representing its canonical capabilities: file management and workflow management. In addition, CAS was augmented by addition of a resource-management component. This third component enables CAS to manage heterogeneous computing by use of diverse resources, including high-performance clusters of computers, commodity computing hardware, and grid computing infrastructures.

CAS is now more easily maintainable, evolvable, and reusable. These components can be used separately or, taking advantage of synergies, can be used together. Other elements of the transformation included addition of a separate Web presentation layer that supports distribution of data products via Really Simple Syndication (RSS) feeds, and

provision for full Resource Description Framework (RDF) exports of metadata.

This work was done by Chris Mattmann, Dana Freeborn, Daniel Crichton, John Hughes, Paul Ramirez, Sean Hardman, and David Woollard of Caltech and Sean Kelly of Northrop Grumman Information Technology for NASA's Jet Propulsion Laboratory. Further information is contained in a TSP (see page 1).

This software is available for commercial licensing. Please contact Karina Edmonds of the California Institute of Technology at (626) 395-2322. Refer to NPO-44883.

🔍 Visualization Component of Vehicle Health Decision Support System

The visualization front-end of a Decision Support System (DSS) also includes an analysis engine linked to vehicle telemetry, and a database of learned models for known behaviors. Because the display is graphical rather than text-based, the summarization it provides has a greater information density on one screen for evaluation by a flight controller. This tool provides a system-level visualization of the state of a vehicle, and "drill-down" capability for more details and interfaces to separate analysis algorithms and sensor data streams.

The system-level view is a 3D rendering of the vehicle, with sensors represented as icons, tied to appropriate positions within the vehicle body and colored to indicate sensor state (e.g., normal, warning, anomalous state, etc.). The sensor data is received via an Information Sharing Protocol (ISP) client that connects to an external server for real-time telemetry. Users can interactively pan, zoom, and rotate this 3D view, as well as select sensors for a detail plot of the associated time series data. Subsets of the plotted data can be selected and sent to an external analysis engine to either search for a similar time series in an historical database, or to detect anomalous events.

The system overview and plotting capabilities are completely general in that they can be applied to any vehicle instrumented with a collection of sensors. This visualization component can interface with the ISP for data streams used by NASA's Mission Control Center at Johnson Space Center. In addition, it can connect to, and display results from, separate analysis engine com-

ponents that identify anomalies or that search for past instances of similar behavior.

This software supports NASA's Software, Intelligent Systems, and Modeling element in the Exploration Systems Research and Technology Program by augmenting the capability of human flight controllers to make correct decisions, thus increasing safety and reliability. It was designed specifically as a tool for NASA's flight controllers to monitor the International Space Station and a future Crew Exploration Vehicle.

This program was written by Joseph Jacob, Michael Turmon, Timothy Stough, and Herbert Siegel of Caltech and Patrick Walter and Cindy Kurt of United Space Alliance for NASA's Jet Propulsion Laboratory. Further information is contained in a TSP (see page 1).

This software is available for commercial licensing. Please contact Karina Edmonds of the California Institute of Technology at (626) 395-2322. Refer to NPO-43952.

➤ Mars Reconnaissance Orbiter Uplink Analysis Tool

This software analyzes Mars Reconnaissance Orbiter (MRO) orbital geometry with respect to Mars Exploration Rover (MER) contact windows, and is the first tool of its kind designed specifically to support MRO-MER interface coordination. Prior to this automated tool, this analysis was done manually with Excel and the UNIX command line. In total, the process would take approximately 30 minutes for each analysis. The current automated analysis takes less than 30 seconds.

This tool resides on the flight machine and uses a PHP interface that does the entire analysis of the input files and takes into account one-way light time from another input file. Input files are copied over to the proper directories and are dynamically read into the tool's interface. The user can then choose the corresponding input files based on the time frame desired for analysis. After submission of the Web form, the tool merges the two files into a single, time-ordered listing of events for both spacecraft. The times are converted to the same reference time (Earth Transmit Time) by reading in a light time file and performing the calculations necessary to shift the time formats. The program also has the ability to vary the size of the keep-out window on the main page of the analysis tool by inputting a custom time for padding each MRO event time. The parameters on the form are read in

and passed to the second page for analysis. Everything is fully coded in PHP and can be accessed by anyone with access to the machine via Web page.

This uplink tool will continue to be used for the duration of the MER mission's needs for X-band uplinks. Future missions also can use the tools to check overflight times as well as potential site observation times. Adaptation of the input files to the proper format, and the window keep-out times, would allow for other analyses. Any operations task that uses the idea of keep-out windows will have a use for this program.

This program was written by Teerapat Khanampornpan, Roy Gladden, Forest Fisher, and Pauline Hwang of Caltech for NASA's Jet Propulsion Laboratory.

This software is available for commercial licensing. Please contact Karina Edmonds of the California Institute of Technology at (626) 395-2322. Refer to NPO-44222.

➤ Problem Reporting System

The Problem Reporting System (PRS) is a Web application, running on two Web servers (load-balanced) and two database servers (RAID-5), which establishes a system for submission, editing, and sharing of reports to manage risk assessment of anomalies identified in NASA's flight projects. PRS consolidates diverse anomaly-reporting systems, maintains a rich database set, and incorporates a robust engine, which allows tracking of any hardware, software, or paper process by configuring an appropriate life cycle. Global and specific project administration and setup tools allow lifecycle tailoring, along with customizable controls for user, e-mail, notifications, and more. PRS is accessible via the World Wide Web for authorized user at most any location.

Upon successful log-in, the user receives a customizable window, which displays time-critical "To Do" items (anomalies requiring the user's input before the system moves the anomaly to the next phase of the lifecycle), anomalies originated by the user, anomalies the user has addressed, and custom queries that can be saved for future use. Access controls exist depending on a user's role as system administrator, project administrator, user, or developer, and then, further by association with user, project, subsystem, company, or item with provisions for business-to-business exclusions, limitations on access according to the covert or overt nature of a given project, all with multiple layers of filtration, as needed. Reporting of metrics is built in. There is a provision

for proxy access (in which the user may choose to grant one or more other users to view screens and perform actions as though they were the user, during any part of a tracking life cycle — especially useful during tight build schedules and vacations to keep things moving). The system also provides users the ability to have an anomaly link to or notify other systems, including QA Inspection Reports, Safety, GIDEP (Government-Industry Data Exchange Program) Alert, Corrective Actions, and Lessons Learned.

The PRS tracking engine was designed as a very extensible and scalable system, able to support additional applications, with future development possibilities already discussed, including Incident Surprise Anomalies (for anomalies occurring during Operations phases of NASA Flight projects), GIDEP and NASA Alerts, and others.

This work was done by Don Potter, Charles Serian, Robert Sweet, Babak Sapir, Enrique Gamez, and David Mays of Caltech for NASA's Jet Propulsion Laboratory.

This software is available for commercial licensing. Please contact Karina Edmonds of the California Institute of Technology at (626) 395-2322. Refer to NPO-40202.

➤ G-Guidance Interface Design for Small Body Mission Simulation

The G-Guidance software implements a guidance and control (G&C) algorithm for small-body, autonomous proximity operations, developed under the Small Body GN&C task at JPL. The software is written in Matlab and interfaces with G-OPT, a JPL-developed optimization package written in C that provides G-Guidance with guaranteed convergence to a solution in a finite computation time with a prescribed accuracy. The resulting program is computationally efficient and is a prototype of an onboard, real-time algorithm for autonomous guidance and control.

Two thruster firing schemes are available in G-Guidance, allowing tailoring of the software for specific mission maneuvers. For example, descent, landing, or rendezvous benefit from a thruster firing at the maneuver termination to mitigate velocity errors. Conversely, ascent or separation maneuvers benefit from an immediate firing to avoid potential drift toward a second body. The guidance portion of this software explicitly enforces user-defined control constraints and thruster silence times while minimizing total fuel usage.

This program is currently specialized to small-body proximity operations, but the underlying method can be generalized to other applications.

This program was written by Behçet Açıkmese, John Carson, and Linh Phan of Caltech for NASA's Jet Propulsion Laboratory.

This software is available for commercial licensing. Please contact Karina Edmonds of the California Institute of Technology at (626) 395-2322. Refer to NPO-44291.

DSN Scheduling Engine

The DSN (Deep Space Network) Scheduling Engine targets all space missions that use DSN services. It allows clients to issue scheduling, conflict identification, conflict resolution, and status requests in XML over a Java Message Service interface. The scheduling requests may include new requirements that represent a set of tracks to be scheduled under some constraints. This program uses a heuristic local search to schedule a variety of schedule requirements, and is being infused into the Service Scheduling Assembly, a mixed-initiative scheduling application.

The engine resolves conflicting schedules of resource allocation according to a range of existing and possible requirement specifications, including optional antennas; start of track and track duration ranges; periodic tracks; locks on track start, duration, and allocated antenna; MSPA (multiple spacecraft per aperture); arraying/VLBI (very long baseline interferometry)/delta DOR (differential one-way ranging); continuous tracks; segmented tracks; gap-to-track ratio; and override or block-out of requirements. The scheduling models now include conflict identification for SOA (start of activity), BOT (beginning of track), RFI (radio frequency interference), and equipment constraints. This software will search through all possible allocations while providing a best-effort solution at any time.

The engine reschedules to accommodate individual emergency tracks in 0.2 second, and emergency antenna downtime in 0.2 second. The software handles doubling of one mission's track requests over one week (to 42 total) in 2.7 seconds. Further tests will be performed in the context of actual schedules.

This program was written by Bradley Clement, Mark Johnston, Allan Wax, and Caroline

Chouinard of Caltech for NASA's Jet Propulsion Laboratory.

This software is available for commercial licensing. Please contact Karina Edmonds of the California Institute of Technology at (626) 395-2322. Refer to NPO-44346.

Replacement Sequence of Events Generator

The soeWINDOW program automates the generation of an ITAR (International Traffic in Arms Regulations)-compliant sub-RSOE (Replacement Sequence of Events) by extracting a specified temporal window from an RSOE while maintaining page header information. RSOEs contain a significant amount of information that is not ITAR-compliant, yet that foreign partners need to see for command details to their instrument, as well as the surrounding commands that provide context for validation. soeWINDOW can serve as an example of how command support products can be made ITAR-compliant for future missions.

This software is a Perl script intended for use in the mission operations UNIX environment. It is designed for use to support the MRO (Mars Reconnaissance Orbiter) instrument team. The tool also provides automated DOM (Distributed Object Manager) storage into the special ITAR-okay DOM collection, and can be used for creating focused RSOEs for product review by any of the MRO teams.

This program was written by Forest Fisher, Daniel Wenkert Roy Gladden, and Teerapat Khanamphornpan of Caltech for NASA's Jet Propulsion Laboratory.

This software is available for commercial licensing. Please contact Karina Edmonds of the California Institute of Technology at (626) 395-2322. Refer to NPO-44392.

Force-Control Algorithm for Surface Sampling

A G-FCON algorithm is designed for small-body surface sampling. It has a linearization component and a feedback component to enhance performance. The algorithm regulates the contact force between the tip of a robotic arm attached to a spacecraft and a surface during sampling. The control algorithm is insensitive to the surface properties, enabling it to

maintain the right contact force for a wide range of surface compliance properties.

The objective of the algorithm is to bring the sampler in contact with the small body surface, and maintain a desired contact force for a prescribed duration of time for sampling. Once the sampling period is over, the control algorithm guides the spacecraft safely away from the surface.

This work was done by Behçet Açıkmese, Marco B. Quadrelli, and Linh Phan of Caltech for NASA's Jet Propulsion Laboratory.

The software used in this innovation is available for commercial licensing. Please contact Karina Edmonds of the California Institute of Technology at (626) 395-2322. Refer to NPO-44377.

Tool for Merging Proposals Into DSN Schedules

A Practical Extraction and Reporting Language (Perl) script called "merge7da" has been developed to facilitate determination, by a project scheduler in NASA's Deep Space Network, of whether a proposal for use of the DSN could create a conflict with the current DSN schedule. Prior to the development of merge7da, there was no way to quickly identify potential schedule conflicts: it was necessary to submit a proposal and wait a day or two for a response from a DSN scheduling facility. By using merge7da to detect and eliminate potential schedule conflicts before submitting a proposal, a project scheduler saves time and gains assurance that the proposal will probably be accepted. merge7da accepts two input files, one of which contains the current DSN schedule and is in a DSN-standard format called "7da."

The other input file contains the proposal and is in another DSN-standard format called "C1/C2." merge7da processes the two input files to produce a merged 7da-format output file that represents the DSN schedule as it would be if the proposal were to be adopted. This 7da output file can be loaded into various DSN scheduling software tools now in use.

This program was written by Teerapat Khanamphornpan, John Kwok, and Jared Call of Caltech for NASA's Jet Propulsion Laboratory.

This software is available for commercial licensing. Please contact Karina Edmonds of the California Institute of Technology at (626) 395-2322. Refer to NPO-44582.



Micromachined Slits for Imaging Spectrometers

Slits can now be made about 100× the precision previously attainable.

NASA's Jet Propulsion Laboratory, Pasadena, California

Slits for imaging spectrometers can now be fabricated to a precision much greater than previously attainable. What makes this possible is a micromachining process that involves the use of microlithographic techniques. This micromachining process supplants a prior machine-shop process.

In the specific application that gave rise to this development, there is a requirement to make imaging-spectrometer slits 27 μm wide and 1.7 cm long. In the prior machine-shop process, the slits were formed by electrical-discharge machining (EDM). The slit widths could not be maintained accurate to within less than about 12 μm , and there was some long-range drift over the 1.7-cm slit lengths. The present micromachining process affords about 100× the precision of the EDM process, with corresponding reductions in the tolerances for slit-width error and long-range drift.

An overview of the micromachining process for fabricating slits consists of the following steps:

1. Grow low-stress silicon nitride via low-pressure chemical vapor deposition (LPCVD) on both sides of a silicon wafer.
2. In a photolithographic subprocess, spin the front-side silicon nitride coated wafer with a photoresist, expose the photoresist through an optical mask to define the opening to be formed, and develop the photoresist to transfer the pattern into the resist.
3. Transfer the photoresist pattern via a dry etch, such as a reactive ion etcher (RIE), through the exposed nitride.
4. Repeat steps 2 and 3 on the backside of the wafer with a pattern to define the opening for the nitride window.
5. Etch through the exposed silicon using an aqueous solution of potas-

sium hydroxide or another suitable strong base.

6. Deposit an opaque, low-stress layer of a suitable metal (e.g., titanium/gold) on both sides.

This work was done by Daniel Wilson, James Kenny, and Victor White of Caltech for NASA's Jet Propulsion Laboratory.

In accordance with Public Law 96-517, the contractor has elected to retain title to this invention. Inquiries concerning rights for its commercial use should be addressed to:

*Innovative Technology Assets Management
JPL*

Mail Stop 202-233

4800 Oak Grove Drive

Pasadena, CA 91109-8099

E-mail: iaoffice@jpl.nasa.gov

Refer to NPO-42378, volume and number of this NASA Tech Briefs issue, and the page number.

Fabricating Nanodots Using Lift-Off of a Nanopore Template

Applications include nano-scale electronic and magnetic devices.

NASA's Jet Propulsion Laboratory, Pasadena, California

A process for fabricating a planar array of dots having characteristic dimensions of the order of several nanometers to several hundred nanometers involves the formation and use of a thin alumina nanopore template on a semiconductor substrate. The dot material is deposited in the nanopores, then the template is lifted off the substrate after the dots have been formed. This process is expected to be a basis for development of other, similar nanofabrication processes for relatively inexpensive mass production of nanometer-scale optical, optoelectronic, electronic, and magnetic devices.

Alumina nanopore templates are self-organized structures that result from anodization of aluminum under appropriate conditions. Alumina nanopore templates have been regarded as attractive for use in fabricating the devices mentioned above, but prior efforts to use alumina nanopore templates for this purpose have not been suc-

cessful. One reason for the lack of success is that the aspect ratios (ratios between depth and diameter) of the pores have been too large: large aspect ratios can result in blockage of deposition and/or can prevent successful lift-off. The development of the present process was motivated partly by a requirement to reduce aspect ratios to values (of the order of 10) for which there is little or no blockage of deposition and attempts at lift-off are more likely to be successful.

The process consists mainly of the following steps:

1. The substrate is cleaned by use of solvents and acids in a subprocess known in the art as Shiraki cleaning.
2. By use of electron-beam evaporation at a deposition rate of 0.5 nm/s, a layer of chromium is deposited to a thickness of 5 nm thick on a silicon substrate and then an aluminum layer 0.4 μm thick, consisting of grains smaller than 0.1

μm , is deposited on the chromium layer. Smallness of the aluminum grains is essential for success.

3. The aluminum layer is anodized at a potential of 10 V in sulfuric acid at a concentration of 0.1 M. The potential of 10 V is considered to be low in the anodization art and results in slow anodization, but the slowness of the anodization is also essential for success.
4. Pores are widened and alumina barrier layers removed by use of phosphoric acid at a concentration of 5 volume percent.
5. The nanodot material is deposited by use of electron-beam evaporation.
6. The alumina template is lifted off by use of a solution of sodium hydroxide at a concentration of 1 M.

This work was done by Eui-Hyeok Yang, Christopher R. Ramsey, Youngsam Bae, and Daniel S. Choi of Caltech for NASA's Jet Propulsion Laboratory. For more information, contact iaoffice@jpl.nasa.gov. NPO-42271

Making Complex Electrically Conductive Patterns on Cloth

Circuit patterns are implemented in tightly woven cloth instead of stitched conductive thread.

Lyndon B. Johnson Space Center, Houston, Texas

A method for automated fabrication of flexible, electrically conductive patterns on cloth substrates has been demonstrated. Products developed using this method, or related prior methods, are instances of a technology known as “e-textiles,” in which electrically conductive patterns are formed in, and on, textiles. For many applications, including high-speed digital circuits, antennas, and radio frequency (RF) circuits, an e-textile method should be capable of providing high surface conductivity, tight tolerances for control of characteristic impedances, and geometrically complex conductive patterns. Unlike prior methods, the present method satisfies all three of these criteria. Typical patterns can include such circuit structures as RF transmission lines, antennas, filters, and other conductive patterns equivalent to those of conventional printed circuits.

E-textiles of various forms have previously been demonstrated, but have typically been hindered by one or more shortfalls. For example, geometrically complex antennas have revealed performance levels that are indistinguish-

able from identical designs on conventional materials. However, construction of the complex geometrical patterns has often been laborious, involving hand-stitching. Another automated method for e-textiles circuit construction uses conductive threads in an embroidery process. However, the embroidered conductive threads do not provide sufficient surface conductivity for many high-speed digital and RF applications. Furthermore, some studies have indicated that the conductive embroidery threads are more subject to breaking than conventional non-conductive embroidery thread.

The present method overcomes the limitations of the prior methods for forming the equivalent of printed circuits on cloth. A typical fabrication process according to the present method involves selecting the appropriate conductive and non-conductive fabric layers to build the e-textile circuit. The present method uses commercially available woven conductive cloth with established surface conductivity specifications. Dielectric constant, loss tangent,

and thickness are some of the parameters to be considered for the non-conductive fabric layers. The circuit design of the conductive woven fabric is secured onto a non-conductive fabric layer using sewing, embroidery, and/or adhesive means. The portion of the conductive fabric that is not part of the circuit is next cut from the desired circuit using an automated machine such as a printed-circuit-board milling machine or a laser cutting machine. Fiducials can be used to align the circuit and the cutting machine. Multilayer circuits can be built starting with the inner layer and using conductive thread to make electrical connections between layers.

This work was done by Andrew Chu, Patrick W. Fink, Justin A. Dobbins, Greg Y. Lin, Robert C. Scully, and Robert Trevino of Johnson Space Center. Further information is contained in a TSP (see page 1).

This invention is owned by NASA, and a patent application has been filed. Inquiries concerning nonexclusive or exclusive license for its commercial development should be addressed to the Patent Counsel, Johnson Space Center, (281) 483-0837. Refer to MSC-24115-1.



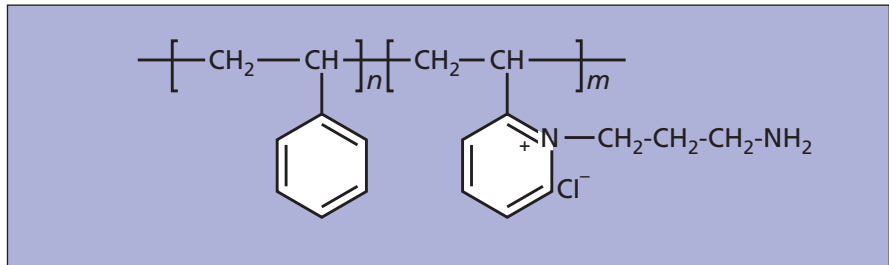
Special Polymer/Carbon Composite Films for Detecting SO₂

These films offer distinct advantages over prior SO₂-sensor materials.

NASA's Jet Propulsion Laboratory, Pasadena, California

A family of polymer/carbon films has been developed for use as sensory films in electronic noses for detecting SO₂ gas at concentrations as low as 1 part per million (ppm). Most previously reported SO₂ sensors cannot detect SO₂ at concentrations below tens of ppm; only a few can detect SO₂ at 1 ppm. Most of the sensory materials used in those sensors (especially inorganic ones that include solid oxide electrolytes, metal oxides, and cadmium sulfide) must be used under relatively harsh conditions that include operation and regeneration at temperatures >100 °C. In contrast, the present films can be used to detect 1 ppm of SO₂ at typical operating temperatures between 28 and 32 °C and can be regenerated at temperatures between 36 and 40 °C.

The basic concept of making sensing films from polymer/carbon composites is not new. The novelty of the present family of polymer/carbon composites lies in formulating the polymer components of these composites specifically to optimize their properties for detecting SO₂. First-principles quantum-mechanical calculations of the energies of binding of SO₂ molecules to various polymer functionalities are used as a guide for selecting polymers and understanding the role of polymer functionalities in sensing.



This Copolymer is a member of the family of polymers suitable for use as components of polymer/carbon composite films for sensing SO₂. The integers *m* and *n* can be chosen by formulation to be in a desired ratio: a typical ratio for the molecular structure shown here is *n/m* = 3/7.

The polymer used in the polymer-carbon composite is a copolymer of styrene derivative units with vinyl pyridine or substituted vinyl pyridine derivative units (see figure). To make a substituted vinyl pyridine for use in synthesizing such a polymer, poly(2-vinyl pyridine) that has been dissolved in methanol is reacted with 3-chloropropylamine that has been dissolved in a solution of methanol. The methanol is then removed to obtain the copolymer. Later, the copolymer can be dissolved in an appropriate solvent with a suspension of carbon black to obtain a mixture that can be cast and then dried to obtain a sensory film.

This work was done by Margie Homer, Margaret Ryan, Shiao-Pin Yen, Adam Kisor, April

Jewell, Abhijit Shevade, Kenneth Manatt, Charles Taylor, Mario Blanco, and William Goddard of Caltech for NASA's Jet Propulsion Laboratory. Further information is contained in a TSP (see page 1).

In accordance with Public Law 96-517, the contractor has elected to retain title to this invention. Inquiries concerning rights for its commercial use should be addressed to:

Innovative Technology Assets Management
JPL

Mail Stop 202-233
4800 Oak Grove Drive
Pasadena, CA 91109-8099
(818) 354-2240

E-mail: iaoffice@jpl.nasa.gov

Refer to NPO-43761, volume and number of this NASA Tech Briefs issue, and the page number.

Nickel-Based Superalloy Resists Embrittlement by Hydrogen

This alloy also exhibits high strength and ductility.

Marshall Space Flight Center, Alabama

A nickel-based superalloy that resists embrittlement by hydrogen more strongly than does nickel alloy 718 has been developed. Nickel alloy 718 is the most widely used superalloy. It has excellent strength and resistance to corrosion as well as acceptably high ductility, and is recognized as the best alloy for many high-temperature applications. However, nickel alloy 718 is susceptible to embrittlement by hydrogen and to delayed failure and reduced tensile properties in gaseous hydrogen. The

greater resistance of the present nickel-based superalloy to adverse effects of hydrogen makes this alloy a superior alternative to nickel alloy 718 for applications that involve production, transfer, and storage of hydrogen, thereby potentially contributing to the commercial viability of hydrogen as a clean-burning fuel.

The table shows the composition of the present improved nickel-based superalloy in comparison with that of nickel alloy 718. This composition was

chosen to obtain high resistance to embrittlement by hydrogen while maintaining high strength and exceptional resistance to oxidation and corrosion. The alloy-design approach followed to arrive at this composition was based on accounting for the simultaneous effects of several additions. The approach included systematic modification of γ -matrix compositions for increased resistance to embrittlement by hydrogen, increasing the volume fraction of the

Element	Proportion in the Present Superalloy	Proportion in Nickel Alloy 718
Ni	Balance	Balance
Fe	24 to 34	17 to 19
Cr	17 to 19	16 to 18
Mo	3.0 to 5.0	2.5 to 3.5
Co	3.0 to 5.0	0.1 to 1.0
V	0.1 to 1.0	—
W	3.0 to 6.0	—
Ti	2.0 to 3.5	0.5 to 1.5
Nb	0.5 to 2.0	4.5 to 6.0
Al	0.1 to 0.5	0.2 to 0.8

Proportions of Chemical Elements in the two alloys are given in weight percentages.

γ' phase, adding γ -matrix-strengthening elements to increase strength, and obtaining precipitate-free grain boundaries. Substantial amounts of chromium and nickel were also included to obtain excellent resistance to oxidation and corrosion. Microstructural stability was maintained through improved solid solubility of the γ ma-

trix along with the addition of alloying elements that retard η -phase precipitation. This alloy represents a material system that greatly extends ranges of composition beyond those of prior nickel-base superalloys that resist embrittlement by hydrogen.

This alloy is first processed by a combination of vacuum induction melting and vac-

uum arc remelting. Typically, the resulting alloy ingot is homogenized at a temperature of 2,100 °C for 24 hours and then hot-rolled in the range of 927 to 1,093 °C into 1.6-cm-thick plates. The plates are subjected to a solution heat treatment at 1,050 °C for 1 hour, followed by aging at 718 °C for 8 hours, then 621 °C for 8 hours.

The most novel property of this alloy is that it resists embrittlement by hydrogen while retaining tensile strength >175 kpsi (>1.2 GPa). This alloy exhibits a tensile elongation of more than 20 percent in hydrogen at a pressure of 5 kpsi (\approx 34 MPa) without loss of ductility. This amount of elongation corresponds to 50 percent more ductility than that exhibited by nickel alloy 718 under the same test conditions.

This work was done by Jonathan Lee of Marshall Space Flight Center and Po-Shou Chen of Illinois Institute of Technology Research Institute. For more information, contact Sammy Nabors, MSFC Commercialization Assistance Lead at sammy.a.nabors@nasa.gov. Refer to MFS -31781-1

Chemical Passivation of Li⁺-Conducting Solid Electrolytes

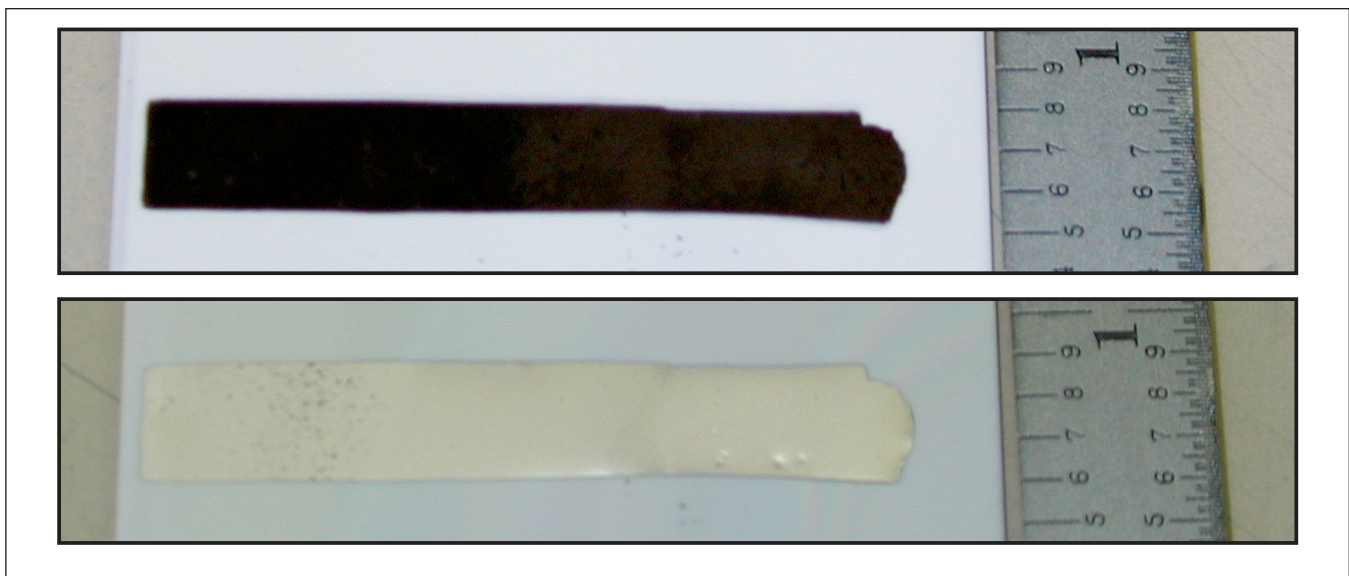
Such passivation could enable long-life lithium rechargeable cells.

NASA's Jet Propulsion Laboratory, Pasadena, California

Plates of a solid electrolyte that exhibits high conductivity for positive lithium ions can now be passivated to prevent them from reacting with metallic lithium. Such passivation could en-

able the construction and operation of high-performance, long-life lithium-based rechargeable electrochemical cells containing metallic lithium anodes. The advantage of this approach, in com-

parison with a possible alternative approach utilizing lithium-ion graphitic anodes, is that metallic lithium anodes could afford significantly greater energy-storage densities.



The Dark Strip in the Upper Photograph is the product of the chemical reaction of a deposited lithium film and an underlying solid-electrolyte plate. The corresponding somewhat shiny strip in the lower photograph is a lithium film deposited on a solid-electrolyte plate coated with LiPON. The dark spots in the Li film contain the reaction product formed at pinholes in the LiPON, where the Li film came into contact with the underlying solid electrolyte. This illustrates the importance of depositing pinhole-free LiPON films to protect solid-electrolyte plates.

A major impediment to the development of such cells has been the fact that the available solid electrolytes having the requisite high Li⁺-ion conductivity are too highly chemically reactive with metallic lithium to be useful, while those solid electrolytes that do not react excessively with metallic lithium have conductivities too low to be useful. The present passivation method exploits the best features of both extremes of the solid-electrolyte spectrum. The basic idea is to coat a higher-conductivity, higher-reactivity solid electrolyte with a lower-conductivity, lower-reactivity solid electrolyte. One can then safely deposit metallic lithium in contact with the lower-reactivity solid electrolyte without incurring the undesired chemical reactions. The thickness of the lower-reactivity electrolyte must be great enough to afford the desired passivation but not so great as to contribute excessively to the electrical resistance of the cell.

The feasibility of this method was demonstrated in experiments on plates of a commercial high-performance solid Li⁺-conducting electrolyte, the composition of which was not disclosed at the time of reporting the information for this article. The lower-conductivity, lower-reactivity solid electrolyte used for passivation was lithium phosphorus oxynitride (commonly abbreviated "LiPON" but more precisely abbreviated Li_xPO_yN_z, where x, y, and z denote numbers that can differ from 1). The solid-electrolyte plates were 50.8-mm square with a thickness of 0.47 mm. Films of Li_{3.3}PO_{3.8}N_{0.22} having thicknesses of the order of 1 μm were deposited on the plates by radio-frequency magnetron sputtering from an Li₃PO₄ target in an atmosphere of N₂. Pt and Cu electrodes were sputtered through a metal shadow mask, and the active lithium anode material was deposited by thermal evaporation through the same mask.

For comparison, some plates were not coated with LiPON and Li was de-

posited directly on them. In those cases, the deposited Li metal reacted immediately with the plates to form dark nonmetallic layers (see upper part of figure) that were electrically nonconductive. In contrast, for the plates that were first coated with LiPON and then with Li, films retained their metallic luster (see lower part of figure) and remained electrically conductive. Test cells containing Li anodes on LiPON-coated plates were constructed and tested by electrochemical impedance spectroscopy and cyclic voltammetry. The coated solid-electrolyte plates were found to support electrochemical plating and stripping of Li metal. The electrical resistances contributed by the LiPON layers were found to be small relative to overall cell impedances.

This work was done by William West, Jay Whitacre, and James Lim of Caltech for NASA's Jet Propulsion Laboratory. Further information is contained in a TSP (see page 1). NPO-40478

Organic/Inorganic Polymeric Composites for Heat-Transfer Reduction

John F. Kennedy Space Center, Florida

Organic/inorganic polymeric composite materials have been invented with significant reduction in heat-transfer properties. Measured decreases of 20–50 percent in thermal conductivity versus that of the unmodified polymer matrix have been attained. These novel composite materials also maintain mechanical properties of the unmodified polymer matrix. The present embodiments are applicable, but not limited to: racing applications, aerospace applications, textile industry, electronic applications, military hardware improve-

ments, and even food service industries. One specific application of the polymeric composition is for use in tanks, pipes, valves, structural supports, and components for hot or cold fluid process systems where heat flow through materials is problematic and not desired.

With respect to thermal conductivity and physical properties, these materials are superior alternatives to prior composite materials. These materials may prove useful as substitutes for metals in some cryogenic applications.

A material of this type can be made from a blend of thermoplastics, elastomers, and appropriate additives and processed on normal polymer processing equipment. The resulting processed organic/inorganic composite can be made into fibers, molded, or otherwise processed into useable articles.

This work was performed by Trent Smith and Martha Williams of Kennedy Space Center. For further information, contact the Kennedy Innovative Partnerships Office at (321) 861-7158. KSC-12890

Composite Cathodes for Dual-Rate Li-Ion Batteries

A battery could have both high charge capacity and high rate capacity.

NASA's Jet Propulsion Laboratory, Pasadena, California

Composite-material cathodes that enable Li-ion electrochemical cells and batteries to function at both high energy densities and high discharge rates are undergoing development. Until now, using commercially available cathode materials, it has been

possible to construct cells that have either capability for high-rate discharge or capability to store energy at average or high density, but not both capabilities. However, both capabilities are needed in robotic, standby-power, and other applications that involve duty cy-

cles that include long-duration, low-power portions and short-duration, high-power portions.

The electrochemically active ingredients of the present developmental composite cathode materials are the following:

- Carbon-coated LiFePO₄, which has a spe-

cific charge capacity of about 160 mA·h/g and has been used heretofore as a high-discharge-rate cathode material; and

- $\text{Li}[\text{Li}_{0.17}\text{Mn}_{0.58}\text{Ni}_{0.25}]\text{O}_2$, which has a specific charge capacity of about 240 mA·h/g and has been used heretofore as a high-energy-density cathode material.

In preparation for fabricating a composite-material cathode in the approach followed thus far in this development effort, the aforementioned electrochemically active ingredients are incorporated into two sub-composites:

- A mixture comprising 10 weight percent of poly(vinylidene fluoride)

[PVDF], 10 weight percent of carbon, and 80 weight percent of carbon-coated LiFePO_4 and,

- A mixture comprising 10 weight percent of PVDF, 10 weight percent of carbon, and 80 weight percent of $\text{Li}[\text{Li}_{0.17}\text{Mn}_{0.58}\text{Ni}_{0.25}]\text{O}_2$.

In the fabrication process, these mixtures are spray-deposited onto an aluminum current collector. While the two mixtures could be spray-deposited simultaneously on the same current-collector area to obtain a single layer comprising a mixture of two sub-composites, electrochemical tests performed thus far

have shown that better charge/discharge performance is obtained when either (1) each mixture is sprayed on a separate area of the current collector or (2) the mixtures are deposited sequentially (in contradistinction to simultaneously) on the same current-collector area so that the resulting composite cathode material consists of two different sub-composite layers.

This work was done by Jay Whitacre, William West, and Ratnakumar Bugga of Caltech for NASA's Jet Propulsion Laboratory. Further information is contained in a TSP (see page 1). NPO-44837



Improved Descent-Rate Limiting Mechanism

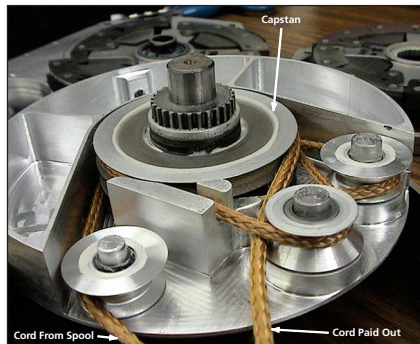
This braking device can be used to capture and slow a moving vehicle.

NASA's Jet Propulsion Laboratory, Pasadena, California

An improved braking cable-payout mechanism has been developed. Like other such mechanisms, this mechanism can be used as a braking or shock-absorbing device for any of a variety of purposes — for example, enabling a person to descend from an upper floor of a burning building at a safe speed, capturing and slowing a moving vehicle, or limiting the shock load generated by opening of a parachute. Whereas other such mechanisms operate at payout speeds that vary with the length of payout, this mechanism operates at approximately constant payout speed, regardless of the length of cord that has already been paid out.

In a prior mechanism of this type, a cord is paid out from a spool on a shaft connected to a centrifugal brake. Because the payout radius on the spool decreases as cord is paid out, the speed decreases by a corresponding amount.

The present mechanism (see figure) includes a spool, a capstan assembly, and centrifugal brakes. The spool is used to store the cord and, unlike in the prior mechanism, is not involved in the primary braking function. That is, the spool operates in such a way that the cord is unwound from the spool at low



The Cord Is Paid Out at Constant Radius from the capstan, which is connected to the centrifugal brake.

tension. The spool is connected to the rest of the mechanism through a constant-torque slip clutch. The clutch must slip in order to pay out the cord.

As the cord leaves the spool, it passes into the capstan assembly, wherein its direction is changed by use of the first of three idler sheaves and it is then routed into the first of three grooves on a capstan. After completing less than a full circle in the first groove, the cord passes over the second idler sheave, which is positioned to enable the cord to make

the transition to the second groove on the capstan. Similarly, a third idler sheave enables the cord to make the transition to the third groove on the capstan. After traveling less than a full circle in the third groove, the cord leaves the capstan along the payout path. The total wrap angle afforded by this capstan-and-idler arrangement is large enough to prevent slippage between the cord and the capstan.

The capstan is connected to a shaft that, in turn, is connected to a centrifugal brake. Hence, the effective payout radius, for purposes of braking, is not the varying radius of the remaining cord on the spool but, rather, the constant radius of the grooves in the capstan. The payout speed is determined primarily by this radius and by the characteristics of the centrifugal brake. Therefore, the payout speed is more nearly constant in this mechanism than in the prior mechanism.

This work was done by Tommaso P. Rivellini, Donald B. Bickler, Bradford Swenson, John Gallon, and Jack Ingle of Caltech for NASA's Jet Propulsion Laboratory. Further information is contained in a TSP (see page 1). NPO-40109

Alignment-Insensitive Lower-Cost Telescope Architecture

This next-generation architecture enables construction of very large telescopes.

Goddard Space Flight Center, Greenbelt, Maryland

This architecture features an active wavefront sensing and control scheme along with methods for measuring the relative positions of the primary to aft optics, such as the secondary mirror, and should enable larger and cheaper telescope architectures needed for future applications. This design overcomes the stability requirements of large telescope primary mirrors.

A wavefront source/sensor is placed at the center of curvature of the primary mirror. The system provides continuous light onto a primary mirror that is retro-reflected onto itself. This allows the

wavefront controller to constantly update the positions of the primary mirror segments (or deformable mirror actuators). For spherical primaries (where replicated mirrors can be used), a spherical source is used. For aspheric primaries, a null is used. The return beam can be analyzed through focus by using established wavefront sensing and control techniques, including prisms for coarse alignment, multi-wavelength interferometry, or phase retrieval. The light can be monochromatic or white light. This same source and sensor can also be used to check out the system during assembly.

Another function of this innovation involves using a concave mirror on the back of the secondary mirror (or other aft optic) that has the same center-of-curvature location (in defocus) as the primary mirror. The two return beams can be aligned next to each other on a detector, or radially on top of each other. This provides a means with which to measure the relative position of the primary to the secondary (or other aft optics), thus allowing for the removal of misalignment of the center-of-curvature source/sensor (meaning it doesn't need precision placement) and also provides

a means with which to monitor the relative alignment over time.

This innovation does not require extremely good thermal stability on the primary mirror and can thus be used in any thermal environment and with cheaper materials. This factor could be critical in enabling the construction of very large telescopes, and provides a means for test-

ing a very large telescope as it is being assembled. In addition to this, the architecture lets one phase (or align) the primary mirror independent of whether a star or scene is in the field. The segmented, spherical primary allows for cost-effective three-meter class (e.g. Midex and Discovery) missions as well as enabling 30-meter telescope solutions

that can be manufactured in a reasonable amount of time. The continuous wavefront sensing and control architecture enables missions for low-Earth-orbit.

This work was done by Lee Feinberg, John Hagopian, Bruce Dean, and Joe Howard for Goddard Space Flight Center. Further information is contained in a TSP (see page 1). GSC-14982-1

⚙️ Micro-Resistojet for Small Satellites

Goddard Space Flight Center, Greenbelt, Maryland

An efficient micro-resistojet has been developed with thrust in the millinewton level, with a specific impulse of approximately 250 seconds and power input of 20 watts or less that is useful for applications of up to 1,000 hours of operation or more. The essential feature of this invention is a gas-carrying tube surrounding a central heating element. The propellant is flashed into vapor and then passes through a narrow annulus between the tube and the heater where it is cracked (in the case of methanol, into CO and

H₂) before being discharged through a de Laval nozzle to produce thrust.

A multi-layer radiation shield around the gas tube minimizes heat loss. Also, if methanol is used as the propellant, the simultaneous heating and cracking does not need an additional device. This unit would be especially useful for small satellites, with mass up to 100 kg, and for delta v up to 500 m/sec, and is suited for use with “green” methanol as the propellant where a specific impulse of 220 seconds is expected. Noble metal alloys are

the optimal materials of construction. While the microresistojet is especially suited to methanol, many other propellants may be used such as water or, in the case of de-orbiting, many other residual liquids onboard the vehicle.

This work was done by Thomas Brogan, Mike Robin, Mary Delichatsios, John Duggan, Kurt Hohman, and Vlad Hruby of Busek Co. Inc. for Goddard Space Flight Center. For further information, contact the Goddard Innovative Partnerships Office at (301) 286-5810. GSC-15053-1

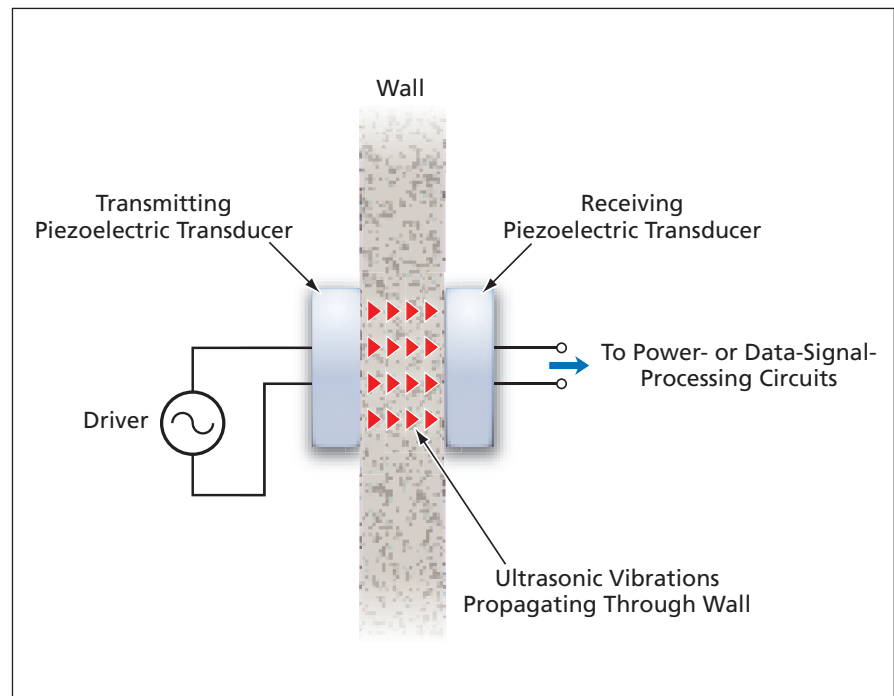
⚙️ Using Piezoelectric Devices To Transmit Power Through Walls

It would not be necessary to make holes in walls for wires.

NASA's Jet Propulsion Laboratory, Pasadena, California

A method denoted wireless acoustic-electric feed-through (WAEF) has been conceived for transmitting power and/or data signals through walls or other solid objects made of a variety of elastic materials that could be electrically conductive or nonconductive. WAEF would make it unnecessary to use wires, optical fibers, tubes, or other discrete wall-penetrating signal-transmitting components, thereby eliminating the potential for structural weakening or leakage at such penetrations. Avoidance of such penetrations could be essential in some applications in which maintenance of pressure, vacuum, or chemical or biological isolation is required.

In a basic WAEF setup (see figure), a transmitting piezoelectric transducer on one side of a wall would be driven at resonance to excite ultrasonic vibrations in the wall. A receiving piezoelectric transducer on the opposite side of the wall would convert the vibrations back to an ultrasonic AC electric signal, which would then be detected and otherwise



Ultrasonic Waves would be used to transmit a power or data signal through a wall.

processed in a manner that would depend on the modulation (if any) applied to the signal and whether the signal was used to transmit power, data, or both.

The basic WAEF concept admits of variations. In one potentially important class of variations, different frequencies (in particular, those of lower- and higher-order resonances) would be used to transmit different signals through a wall in the same direction or in opposite directions. For example, an exterior ultrasonic transducer on a vessel could be excited at the fundamental resonance frequency to transmit power through the wall to an interior ultrasonic transducer to activate instrumentation inside the ves-

sel, while the interior ultrasonic transducer could be excited at the frequency of a higher-order resonance to transmit data signals from the interior instrumentation to an external computer.

An electromechanical-network model has been derived as a computationally efficient means of analyzing and designing a WAEF system. This model is a variant of a prior model, known in the piezoelectric-transducer art as Mason's equivalent-circuit model, in which the electrical and mechanical dynamics, including electromechanical couplings, are expressed as electrical circuit elements that can include inductors, capacitors, and lumped-parameter

complex impedances. The real parts of the complex impedances are used to account for dielectric, mechanical, and coupling losses in all components (including all piezoelectric-transducer, wall, and intermediate material layers). In an application to a three-layer piezoelectric structure, this model was shown to yield the same results as do solutions of the wave equations of piezoelectricity and acoustic propagation in their full complexity.

This work was done by Stewart Sherrit, Yoseph Bar-Cohen, and Xiaoqi Bao of Caltech for NASA's Jet Propulsion Laboratory. For further information, contact iaoffice@jpl.nasa.gov. NPO-41157

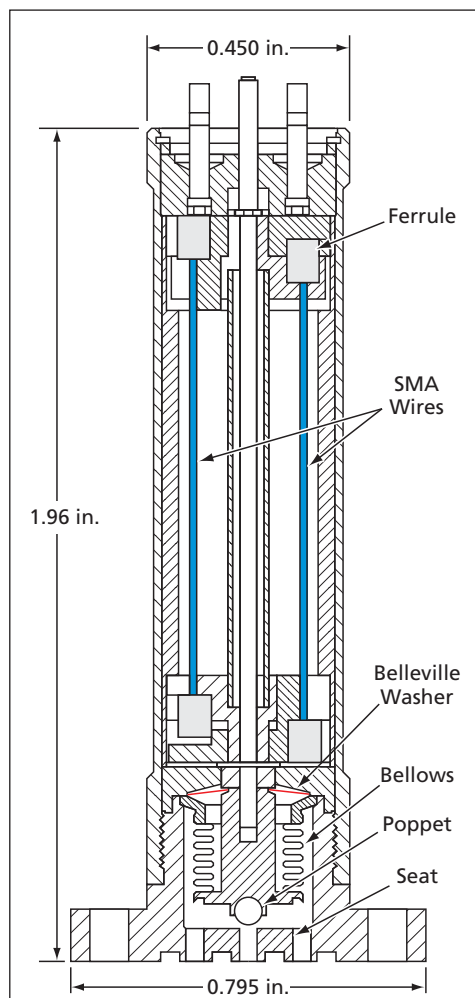
⚙️ Miniature Latching Valve

This valve remains either open or closed when power is not supplied.

Goddard Space Flight Center, Greenbelt, Maryland

A miniature latching valve has been invented to satisfy a need for an electrically controllable on/off pneumatic valve that is lightweight and compact and remains in the most recently commanded open or closed state when power is not supplied. The valve (see figure) includes a poppet that is moved into or out of contact with a seat to effect closure or opening, respectively, of the flow path. Motion of the poppet is initiated by electrical heating of one of two opposing pairs of nickel/titanium shape-memory alloy (SMA) wires above their transition temperature: heated wires contract to their "remembered" length, applying tension to pull the poppet toward or away from the seat. A latch consisting mainly of a bistable Belleville washer (a conical spring) made of a hardened stainless steel operates between two stable positions corresponding to the fully closed or fully open state, holding the poppet in one of these positions when power is not applied to either pair of SMA wires.

The reason for using SMA wires is that in comparison with other linear actuators of the same mass and size, SMA wires produce more work output. The light weight and compactness of the SMA-wire actuators and the Belleville-washer latch make it possible for this valve to be smaller and less massive than are prior valves of comparable performance.



The **Miniature Latching Valve**, shown here in the open state, is actuated between the open and closed states by means of the SMA wires and the Belleville washer.

To obtain maximum actuation force and displacement, the SMA wires must be kept in tension. The mounting fixtures at the ends of the wires must support large tensile stresses without creating stress concentrations that would limit the fatigue lives of the wires. An earlier design provided for each wire to be crimped in a conical opening with a conical steel ferrule that was swaged into the opening to produce a large, uniformly distributed holding force. In a subsequent design, the conical ferrule was replaced with a larger crimped cylindrical ferrule depicted in the figure.

A major problem in designing the valve was to protect the SMA wires from a bake-out temperature of 300 °C. The problem was solved by incorporating the SMA wires into an actuator module that is inserted into a barrel of the valve body and is held in place by miniature clip rings.

This work was done by A. David Johnson of TiNi Alloy Co. and Glendon M. Benson of Aker Industries for Goddard Space Flight Center.

In accordance with Public Law 96-517, the contractor has elected to retain title to this invention. Inquiries concerning rights for its commercial use should be addressed to:

*TiNi Alloy Company
1619 Neptune Drive
San Leandro, CA 94577*

Refer to GSC-14881-1, volume and number of this NASA Tech Briefs issue, and the page number.



Apparatus for Sampling Surface Contamination

Liquid suspensions of samples can be dispensed systematically into analytical instruments.

Marshall Space Flight Center, Alabama

An apparatus denoted a swab device has been developed as a convenient means of acquiring samples of contaminants from surfaces and suspending the samples in liquids. (Hereafter, the liquids can be dispensed, in controlled volumes, into scientific instruments for analysis of the contaminants.) The swab device is designed so as not to introduce additional contamination and to facilitate, simplify, and systematize the dispensing of controlled volumes of liquid into analytical instruments.

The use of currently commercially available contamination-sampling devices involves significant mechanical manipulation of samples and liquids, and there is no provision for systematic dispensing of controlled volumes of liquid into analytical instruments: A typical use involves wiping a surface of interest with a standard implement resembling a cotton swab. The implement is then placed into a volume containing the liquid in which the sample is to be suspended. Ultimately, the liquid must be extracted from this volume and dispensed into an analytical instrument by use of a pipette. The swab device is a single apparatus into which are combined

all the equipment and materials needed for sampling surface contamination. The swab device contains disposable components stacked together on a non-disposable dispensing head. One of the disposable components is a supply cartridge holding a sufficient volume of liquid for one complete set of samples. (The liquid could be clean water or another suitable solvent, depending on the application.) This supply of liquid is sealed by Luer valves.

At the beginning of a sampling process, the user tears open a sealed bag containing the supply cartridge. A tip on the nondisposable dispensing head is engaged with a Luer valve on one end of the supply cartridge and rotated, locking the supply cartridge on the dispensing head and opening the valve. A bag containing a disposable swab tip is opened, and the end of the supply cartridge opposite the aforementioned end is engaged with the swab tip and rotated, opening a valve.

The swab tip includes a fabric swab that is wiped across the surface of interest to acquire a sample. A sealed bag containing a disposable dispensing tip (not to be confused with the non-dispos-

able dispensing head) is then opened, and the swab tip is pushed into the dispensing tip until seated. The dispensing head contains a piston that passes through a spring-loaded lip seal. The air volume displaced by this piston forces the liquid out of the supply cartridge, over the swab, and into the dispensing tip. The piston is manually cycled to enforce oscillation of the air volume and thereby to cause water to flow to wash contaminants from the swab and cause the resulting liquid suspension of contaminants to flow into the dispensing tip. After cycling several times to ensure adequate mixing, liquid containing the suspended contaminant sample is dispensed through the dispensing tip in 25- μ L increments into an analytical instrument. The disposable components are then removed from the dispensing head. Thereafter, the dispensing head can be reused with a fresh set of disposable components.

This work was done by Mark Wells of UAH for Marshall Space Flight Center. For further information, contact Sammy Nabors, MSFC Commercialization Assistance Lead, at sammy.a.nabors@nasa.gov. Refer to MFS-32560-1.

Novel Species of Non-Spore-Forming Bacteria

One new bacterial species was discovered in a regenerative enclosed life-support module air system.

NASA's Jet Propulsion Laboratory, Pasadena, California

While cataloging cultivatable microbes from the airborne biological diversity of the atmosphere of the Regenerative Enclosed life-support Module Simulator (REMS) system at Marshall Space Flight Center, two strains that belong to one novel bacterial species were isolated. Based on 16S rRNA gene sequencing and the unique morphology and the taxonomic characteristics of these strains, it is shown that they belong to the family *Intrasporangiaceae*, related to the genus *Tetrasphaera*, with phylogenetic distances from any validly described species of the

genus *Tetrasphaera* ranging from 96.71 to 97.76 percent.

The fatty acid profile supported the affiliation of these novel strains to the genus *Tetrasphaera* except for the presence of higher concentrations of octadecenoic acid ($C_{18:0}$) and *cis*-9-octadecenoic acid ($C_{18:1}$), which discriminates these strains from other valid species. In addition, DNA-DNA hybridization studies indicate that these strains belong to a novel species that could be readily distinguished from its nearest neighbor, *Tetrasphaera japonica* AMC

5116^T, with less than 20 percent DNA relatedness. Physiological and biochemical tests show few phenotypic dissimilarities, but genotypic analysis allowed the differentiation of these gelatin-liquefying strains from previously reported strains. The name *Tetrasphaera remsis* sp. Nov. is proposed with the type strain 3-M5-R-4^T (=ATCC BAA-1496^T=CIP 109413^T). The GenBank/EMBL/DBJ accession numbers for the 16S rRNA gene sequence are DQ447774 and EF028236 for the strains 3-M5-R-4^T and 3-M5-R-7, respectively.

The cells are Gram-positive, non-motile, cocci, in tetrad arrangement and clusters. Spore formation is not observed. The colonies are beige in color and convex with a glossy surface. The organisms are aerobic chemoheterotrophic in nature. They do not reduce nitrate to nitrite. They show no anaerobic growth and do not ferment glucose. They are gelatin-liquefying and esculin hydrolyzed. Catalase and β -galactosidase are produced. The cells use D-glucose, D-mannose, D-mannitol, D-maltose, N-acetyl-glucosamine, and malate. Tests show that the

cells do not assimilate the following compounds: L-arabinose, gluconate, capric acid, adipic acid, phenyl acetic acid, or citrate. Growth occurs at 15 to 45 °C and at pH 6–9. The optimal growth temperature and pH are 25 °C and 7, respectively.

No species of *Tetrashpaera* has ever been isolated from airborne samples. Previous discoveries have come from soil and activated sludge samples. As other species of this genus have demonstrated enhanced biological phosphorus removal activity, further tests are required to determine if this newly

discovered species would have bioremediation applications.

This work was done by Shariff Osman, Christine Moissl, Naofumi Hosoya, and Kasthuri Venkateswaran of the Biotechnology and Planetary Protection Group at Jet Propulsion Laboratory; Ariane Briegel of Caltech; Masataka Satomi of the National Research Institute of Fisheries Science, Fisheries Research Agency-Japan; and Shanmugam Mayilraj of MTCC Institute of Microbial Technology-India for NASA's Jet Propulsion Laboratory. For more information, contact iaoffice@jpl.nasa.gov. NPO-45092

Chamber for Aerosol Deposition of Bioparticles

Standard coupons can be covered with reproducible areal concentrations of bioparticles.

NASA's Jet Propulsion Laboratory, Pasadena, California

The laboratory apparatus shown in the figure is a chamber for aerosol deposition of bioparticles on surfaces of test coupons. It is designed for primary use in inoculating both flat and three-dimensional objects with approximately reproducible, uniform dispersions of bacterial spores of the genus *Bacillus* so that the objects could be used as standards for removal of the spores by quantitative surface sampling and/or cleaning processes. The apparatus is also designed for deposition of particles other than bacterial spores, including fungal spores, viruses, bacteriophages, and standard micron-sized beads. The novelty of the apparatus lies in the combination of a controllable nebulization system with a settling chamber large enough to contain a significant number of test coupons. Several companies market other nebulizer systems, but none are known to include chambers for deposition of bioparticles to mimic the natural fallout of bioparticles.

The nebulization system is an expanded and improved version of commercially available aerosol generators that include nebulizers and drying columns. In comparison with a typical commercial aerosol generator, this system includes additional, higher-resolution flowmeters and an additional pres-



This **Bioparticle-Deposition Chamber** is sized to fit on a laboratory bench and to fit within a standard class-II biological safety cabinet.

sure regulator. Also, unlike a typical commercial aerosol generator, it includes stopcocks for separately controlling flows of gases to the nebulizer and drying column.

To maximize the degree of uniformity of dispersion of bioaerosol, the chamber is shaped as an axisymmetrical cylinder and the aerosol generator is positioned centrally within the chamber and aimed upward like a fountain. In order to mini-

mize electric charge associated with the aerosol particles, the drying column is made of aluminum, the drying column is in direct contact with an aluminum base plate, and three equally spaced ^{210}Po anti-static strips are located at the exit end of the drying column. The sides and top of the chamber are made of an acrylic polymer; to prevent accumulation of electric charge on them, they are spray-coated with an anti-static material. During use, the base plate and the sides and top of the chamber are grounded as a further measure to minimize the buildup of electric charge.

This work was done by Roger Kern and Larry Kirschner of Caltech for NASA's Jet Propulsion Laboratory. Further information is contained in a TSP (see page 1).

In accordance with Public Law 96-517, the contractor has elected to retain title to this invention. Inquiries concerning rights for its commercial use should be addressed to:

*Innovative Technology Assets Management
JPL*

*Mail Stop 202-233
4800 Oak Grove Drive
Pasadena, CA 91109-8099
(818) 354-2240*

E-mail: iaoffice@jpl.nasa.gov

Refer to NPO-42191, volume and number of this NASA Tech Briefs issue, and the page number.



Hyperspectral Sun Photometer for Atmospheric Characterization and Vicarious Calibrations

Data acquired by such devices are used in atmospheric, pollution, and solar energy studies.

Stennis Space Center, Mississippi

A hyperspectral sun photometer and associated methods have been developed and demonstrated. Sun photometers are used to measure total (global), direct, and diffuse at-surface solar irradiance. The data acquired by sun photometers are used in atmospheric, pollution, and solar energy studies. In addition, the data acquired by sun photometers are used for radiometric vicarious calibration of optical remote-sensing systems. Sun photometer measurements at various wavelengths can be analyzed to estimate molecular scattering, aerosol extinction, and columnar concentrations of water vapor, ozone, and trace gases in the atmosphere.

Accurate sun photometer calibration is critical to properly measure the solar irradiance and characterize the atmosphere. Traditional sun photometer calibration requires solar observations over several hours. This approach can be impractical and inadequate, particularly in places where the atmosphere is harsh and/or its optical characteristics are variable. In contrast, the procedures for operating this photometer entail less data acquisition time and embody a more direct approach to calibration. The scientific value of the measurement data produced by this instrument is not adversely affected by at-

mospheric instability. In addition, this instrument yields hyperspectral data covering a large spectral range (350–2,500 nm) not available from most traditional sun photometers.

The hyperspectral sun photometer components include (1) a commercially available spectroradiometer that has been calibrated in a laboratory according to standards traceable to the National Institute of Standards and Technology and (2) a commercially available reflectance standard panel that exhibits nearly Lambertian 99-percent reflectance. The spectroradiometer is positioned above, and aimed downward at, the panel. The procedure for operating this instrument calls for a series of measurements: one in which the panel is fully illuminated by the sun, one in which a shade is positioned between the panel and the sun, and two in which the shade is positioned to cast a shadow to either side of the panel. The total sequence of measurements can be performed in less than a minute.

From these measurements, the total radiance, the diffuse radiance, and the direct solar radiance are calculated. The direct solar irradiance is calculated from the direct solar radiance and the known reflectance factor of the panel as a func-

tion of the solar zenith angle. Atmospheric characteristics are estimated from the optical depth at various wavelengths calculated from (1) the direct solar irradiance obtained as described above, (2) the air mass along a column from the measurement position to the Sun, and (3) the top-of-atmosphere solar irradiance.

The instrumentation used to implement the sun photometer is the same as that used to characterize targets used in radiometric vicarious calibrations. Utilizing this type of sun photometer thus reduces the amount of instrumentation and labor required to perform these studies.

This work was done by Mary Pagnutti, Robert Ryan, and Kara Holekamp of Science Systems and Applications, Inc. for Stennis Space Center.

Inquiries concerning rights for the commercial use of this invention should be addressed to:

Science Systems and Applications, Inc.

Stennis Space Center

Building 1105

Stennis Space Center, MS 39529

(228) 688-2135

E-mail: Mary.Pagnutti-1@nasa.gov

Refer to SSC-00252, volume and number of this NASA Tech Briefs issue, and the page number.

Dynamic Stability and Gravitational Balancing of Multiple Extended Bodies

NASA's Jet Propulsion Laboratory, Pasadena, California

Feasibility of a non-invasive compensation scheme was analyzed for precise positioning of a massive extended body in free fall using gravitational forces influenced by surrounding source masses in close proximity. The N -body problem of classical mechanics is a paradigm used to gain insight into the physics of the equivalent N -body problem subject to control forces.

The analysis addressed how a number of control masses move around the proof mass so that the proof mass position can be accurately and remotely compensated when exogenous disturbances are acting on it, while its sensitivity to gravitational waves remains unaffected. Past methods to correct the dynamics of the proof mass have considered active electrostatic or capacitive methods, but the possibility of

stray capacitances on the surfaces of the proof mass have prompted the investigation of other alternatives, such as the method presented in this paper.

While more rigorous analyses of the problem should be carried out, the data show that, by means of a combined feedback and feed-forward control approach, the control masses succeeded in driving the proof mass along the speci-

fied trajectory, which implies that the proof mass can, in principle, be balanced via gravitational forces only while external perturbations are acting on it. This concept involves the dynamic stability of a group of massive objects interact-

ing gravitationally under active control, and can apply to drag-free control of spacecraft during missions, to successor gravitational wave space borne sensors, or to any application requiring flying objects to be precisely controlled in posi-

tion and attitude relative to another body via gravitational interactions only.

This work was done by Marco Quadrelli of Caltech for NASA's Jet Propulsion Laboratory. For more information, contact iaoffice@jpl.nasa.gov. NPO-42166



Simulation of Stochastic Processes by Coupled ODE-PDE

A document discusses the emergence of randomness in solutions of coupled, fully deterministic ODE-PDE (ordinary differential equations-partial differential equations) due to failure of the Lipschitz condition as a new phenomenon. It is possible to exploit the special properties of ordinary differential equations (represented by an arbitrarily chosen, dynamical system) coupled with the corresponding Liouville equations (used to describe the evolution of initial uncertainties in terms of joint probability distribution) in order to simulate stochastic processes with the proscribed probability distributions. The important advantage of the proposed approach is that the simulation does not require a random-number generator.

This work was done by Michail Zak of Caltech for NASA's Jet Propulsion Laboratory. Further information is contained in a TSP (see page 1). NPO-45241

Cluster Inter-Spacecraft Communications

A document describes a radio communication system being developed for exchanging data and sharing data-processing capabilities among spacecraft flying in formation. The system would establish a high-speed, low-latency, deterministic loop communication path connecting all the spacecraft in a cluster. The system would be a wireless version of a ring bus that complies with the Institute of Electrical and Electronics Engineers (IEEE) standard 1393 (which pertains to a spaceborne fiber-optic data bus enhancement to the IEEE standard developed at NASA's Jet Propulsion Laboratory). Every spacecraft in the cluster would be equipped with a ring-bus radio transceiver. The identity of a spacecraft would be established upon connection into the ring bus, and the spacecraft could be at any location in the ring communication sequence.

In the event of failure of a spacecraft, the ring bus would reconfigure itself, bypassing a failed spacecraft. Similarly, the ring bus would reconfigure itself to accommodate a spacecraft newly added to the cluster or newly enabled or re-enabled. Thus, the ring bus would be scalable and

robust. Reliability could be increased by launching, into the cluster, spare spacecraft to be activated in the event of failure of other spacecraft.

This work was done by Brian Cox of Caltech for NASA's Jet Propulsion Laboratory. Further information is contained in a TSP (see page 1).

In accordance with Public Law 96-517, the contractor has elected to retain title to this invention. Inquiries concerning rights for its commercial use should be addressed to:

*Innovative Technology Assets Management
JPL*

Mail Stop 202-233

4800 Oak Grove Drive

Pasadena, CA 91109-8099

E-mail: iaoffice@jpl.nasa.gov

Refer to NPO-45379, volume and number of this NASA Tech Briefs issue, and the page number.

Genetic Algorithm Optimizes Q-LAW Control Parameters

A document discusses a multi-objective, genetic algorithm designed to optimize Lyapunov feedback control law (Q-law) parameters in order to efficiently find Pareto-optimal solutions for low-thrust trajectories for electronic propulsion systems. These would be propellant-optimal solutions for a given flight time, or flight time optimal solutions for a given propellant requirement. The approximate solutions are used as good initial solutions for high-fidelity optimization tools. When the good initial solutions are used, the high-fidelity optimization tools quickly converge to a locally optimal solution near the initial solution.

Q-law control parameters are represented as real-valued genes in the genetic algorithm. The performances of the Q-law control parameters are evaluated in the multi-objective space (flight time vs. propellant mass) and sorted by the non-dominated sorting method that assigns a better fitness value to the solutions that are dominated by a fewer number of other solutions. With the ranking result, the genetic algorithm encourages the solutions with higher fitness values to participate in the reproduction process, improving the

solutions in the evolution process. The population of solutions converges to the Pareto front that is permitted within the Q-law control parameter space.

This work was done by Seungwon Lee, Paul von Allmen, Anastassios Petropoulos, and Richard Terrile of Caltech for NASA's Jet Propulsion Laboratory. Further information is contained in a TSP (see page 1).

The software used in this innovation is available for commercial licensing. Please contact Karina Edmonds of the California Institute of Technology at (626) 395-2322. Refer to NPO-44489.

Low-Impact Mating System for Docking Spacecraft

A document describes a low-impact mating system suitable for both docking (mating of two free-flying spacecraft) and berthing (in which a robot arm in one spacecraft positions an object for mating with either spacecraft). The low-impact mating system is fully androgynous: it mates with a copy of itself, i.e., all spacecraft and other objects to be mated are to be equipped with identical copies of the system. This aspect of the design helps to minimize the number of unique parts and to standardize and facilitate mating operations. The system includes a closed-loop feedback control subsystem that actively accommodates misalignments between mating spacecraft, thereby attenuating spacecraft dynamics and mitigating the need for precise advance positioning of the spacecraft.

The operational characteristics of the mating system can be easily configured in software, during operation, to enable mating of spacecraft having various masses, center-of-gravity offsets, and closing velocities. The system design provides multi-fault tolerance for critical operations: for example, to ensure unmating at a critical time, a redundant unlatching mechanism and two independent pyrotechnic release subsystems are included.

This work was done by James L. Lewis and Brandon Robertson of Johnson Space Center and Monty B. Carroll, Thang Le, and Ray Morales of Lockheed Martin Corp. Further information is contained in a TSP (see page 1).

This invention is owned by NASA, and a patent application has been filed. Inquiries concerning nonexclusive or exclusive license for its commercial development should be ad-

dressed to the Patent Counsel, Johnson Space Center, (281) 483-0837. Refer to MSC-23933-1.

Non-Destructive Evaluation of Materials via Ultraviolet Spectroscopy

A document discusses the use of ultraviolet spectroscopy and imaging for the non-destructive evaluation of the degree of cure, aging, and other properties of resin-based composite materials. This method can be used in air, and is portable for field use. This method operates in reflectance, absorbance, and luminescence modes.

The ultraviolet source is used to illuminate a composite surface of interest. In reflectance mode, the reflected response is acquired via the imaging system or via the spectrometer. The spectra are analyzed for organic compounds (conjugated organics) and inorganic compounds (semiconducting band-edge states; luminescing defect states such as silicates, used as adhesives for composite aerospace applications; and metal oxides commonly used as thermal coating paints on a wide range of spacecraft). The spectra are compared with a database for variation in conjugation, substitution, or length of molecule (in the case of organics) or band edge position (in the case of inorganics).

This approach is useful in the understanding of material quality. It lacks the precision in defining the exact chemical structure that is found in other materials analysis techniques, but it is advantageous over methods such as nuclear magnetic resonance, infrared spectroscopy, and chromatography in that it can be used in the field to assess significant changes in chemical structure that may be linked to concerns associated with weaknesses or variations in structural integrity, without disassembly of or destruction to the structure of interest.

This work was done by Betsy Pugel of Goddard Space Flight Center. Further information is contained in a TSP (see page 1).GSC-15338-1

Gold-on-Polymer-Based Sensing Films for Detection of Organic and Inorganic Analytes in the Air

A document discusses gold-on-polymer as one of the novel sensor types developed for part of the sensor development task. Standard polymer-carbon composite sensors used in the JPL Electronic Nose (ENose) have been modified by evaporating 15 nm of metallic gold on the surface. These sensors have been shown to respond to alcohols, aromatics, ammonia, sulfur dioxide, and elemental mercury in the parts-per-million and parts-per-billion concentration ranges in humidified air.

The results have shown good sensitivity of these films operating under mild conditions (operating temperatures 23–28 °C and regeneration temperature up to 40 °C). This unique sensor combines the diversity of polymer sensors for chemical sensing with their response to a wide variety of analytes with the specificity of a gold sensor that shows strong reaction/binding with selected analyte types, such as mercury or sulfur.

This work was done by Kenneth Manatt of Santa Barbara Research and Margie Homer, Margaret Ryan, Adam Kisor, Abhijit Shevade, April Jewell, and Hanying Zhou of Caltech for NASA's Jet Propulsion Laboratory. Further information is contained in a TSP (see page 1).

In accordance with Public Law 96-517, the contractor has elected to retain title to this invention. Inquiries concerning rights for its commercial use should be addressed to:

*Innovative Technology Assets Management
JPL
Mail Stop 202-233
4800 Oak Grove Drive
Pasadena, CA 91109-8099*

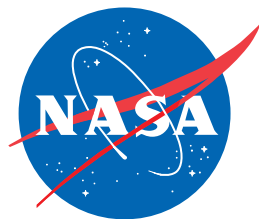
*E-mail: iaoffice@jpl.nasa.gov
Refer to NPO-44997, volume and number of this NASA Tech Briefs issue, and the page number.*

Quantum-Inspired Maximizer

A report discusses an algorithm for a new kind of dynamics based on a quantum-classical hybrid-quantum-inspired maximizer. The model is represented by a modified Madelung equation in which the quantum potential is replaced by different, specially chosen “computational” potential. As a result, the dynamics attains both quantum and classical properties: it preserves superposition and entanglement of random solutions, while allowing one to measure its state variables, using classical methods. Such optimal combination of characteristics is a perfect match for quantum-inspired computing. As an application, an algorithm for global maximum of an arbitrary integrable function is proposed. The idea of the proposed algorithm is very simple: based upon the Quantum-Inspired Maximizer (QIM), introduce a positive function to be maximized as the probability density to which the solution is attracted. Then the larger value of this function will have the higher probability to appear.

Special attention is paid to simulation of integer programming and NP-complete problems. It is demonstrated that the problem of global maximum of an integrable function can be found in polynomial time by using the proposed quantum-classical hybrid. The result is extended to a constrained maximum with applications to integer programming and TSP (Traveling Salesman Problem).

*This work was done by Michail Zak of Caltech for NASA's Jet Propulsion Laboratory. Further information is contained in a TSP (see page 1).
NPO-45458*



National Aeronautics and
Space Administration